Oxidative desulfurization of tire pyrolysis oil over molybdenum heteropolyacid supported mesoporous catalysts

A thesis submitted to the College of Graduate and Postdoctoral Studies

In partial fulfillment of the requirements for the

Degree of Master of Science

In the Department of Chemical and Biological Engineering

University of Saskatchewan

Saskatoon, SK

Canada

By

Jasmine Kaur

PERMISSION TO USE

In presenting this thesis in partial fulfillment of the requirements for a Master of Science degree from the University of Saskatchewan, I agree that the libraries of this University may make it freely available for inspection. I further agree that permission for copying of this thesis in any manner, in whole or in part, for scholarly purposes may be granted by Dr. Ajay Dalai and Dr. John Adjaye, who supervised my thesis work, or in their absence, by the Head of the Department or the Dean of the College of Engineering. It is understood that any copying or publication or use of this thesis or parts thereof for financial gain is prohibited and shall not be allowed without my written permission. It is also understood that due recognition shall be given to me and to the University of Saskatchewan in any scholarly use which may be made of any material in my thesis.

Requests for permission to copy or to make other uses of materials in this thesis/dissertation in whole or part should be addressed to:

Head of the Department

Chemical and Biological Engineering

University of Saskatchewan

57 Campus Drive

Saskatoon, Saskatchewan

S7N 5A9 Canada

OR

Dean

College of Graduate and Postdoctoral Studies

University of Saskatchewan

116 Thorvaldson Building, 110 Science Place

Saskatoon, Saskatchewan S7N 5C9 Canada

ABSTRACT

Pyrolytic oil derived from waste tires consists of high sulfur content in the range of 7000–9000 ppm. To use as transportation fuels, its sulfur content needs to be lowered to 10–15 ppm. Though conventional hydrodesulfurization is suitable for sulfur removal in tire pyrolytic oil, its high cost provides the avenue for alternative desulfurization technologies to be explored. In this study, oxidative desulfurization, a low-cost technology was explored for desulfurization of tire pyrolytic oil at mild process conditions. Two categories of Ti-incorporated mesoporous supports with 20 wt.% loaded heteropoly molybdic acid catalysts (HPMo/Ti-Al$_2$O$_3$ and HPMo/Ti-TUD-1) were developed and tested for oxidative desulfurization of tire pyrolytic oil. Catalysts were characterized by X-ray diffraction, BET-N$_2$ physisorption, and X-ray photoelectron spectroscopy. The surface acidity of catalysts was studied by temperature-programmed desorption of NH$_3$ and pyridine FTIR analyses. The presence of titanium in catalysts was found to promote the ODS activity of phosphomolybdic acid. Ti-TUD-1 supported catalysts performed better than Ti-Al$_2$O$_3$ supported catalysts as the former retains its keggin structure from phosphomolybdic acid. Hydrogen peroxide and cumene peroxide were found to be better oxidants than tert-butyl hydroperoxide for ODS of tire pyrolytic oil. Process parameter optimization study along with the catalyst regeneration study was carried out with phosphomolybdic acid on Ti-TUD-1 (Ti/Si= 0.025) catalyst, which was found to be most suitable for the ODS process. ANOVA statistical analysis was carried out to elucidate the significance of process parameters. Kinetic study for oxidative desulfurization was confirmed to be a pseudo-first-order reaction over HPMo/Ti-TUD-1 catalyst.

Keywords: Tire pyrolysis oil, oxidative desulfurization, phosphomolybdic acid, Ti-TUD-1, Ti-Al$_2$O$_3$

ACKNOWLEDGEMENT

TABLE OF CONTENTS

LIST OF TABLES

LIST OF FIGURES

LIST OF ABBREVIATIONS

HDS	Hydrodesulfurization
ODS	Oxidative desulfurization
TPO	Tire pyrolysis oil
DBT	Dibenzothiophene
ppm	Parts per million (by wt%)
BT	Benzothiophene
TBHP	Tert-butyl hydroperoxide
HPMo	Heteropolymolybdic acid
HT-LGO	Hydrotreated light gas oil
BET	Brunauer-Emmett-Teller
BJH	Barret-Joyner-Halenda
FTIR	Fourier Transform Infrared spectroscopy
XRD	X-ray Diffraction
TPD	Temperature-Programmed desorption
XPS	X-ray photoelectron spectroscopy
Cat/Oil	Amount of catalyst in oil
O/S	Oxidant/Sulfur

Chapter 1: Introduction

1.1 Research Background

The U.S. Energy Information Administration (EIA) anticipates a rise of global oil consumption by 3.7 million b/d (barrel(s) per day) in 2022 and further projected an increasing trend for the subsequent years ("Short-Term Energy Outlook", 2021). To meet the demands of the anticipated upsurge in global oil consumption, alternate resources such as the conversion of waste energy will play a critical role in the future energy outlook. With the growing automotive industry, the huge quantity of waste tires produced in the world will certainly increase in the future (Juma *et al.,* 2007). Hence, researchers are trying to valorize scrap tires into drop-in fuel by various kinds of procedures and techniques. The global tire market is expecting a compound annual growth rate (CAGR) of around 4 % throughout 2021-2026 ("Worldwide Tire Industry", 2021). The Canadian tire market was observed around CAD 5 billion in 2019 and is expected to grow by approximately 4 % during 2021-2026 with the hike of CAD 6 billion industry by 2026 due to the increase of industrialization ("Automotive", 2021).

Typically, at the end of their lives, waste tires are discarded into landfills where they pose health and fire hazards due to their non-biodegradable nature. This year, (February 12, 2021) marked exactly 31 years after the traumatic tire fire that burned a pile of 14 million scrap tires for 17 days in Hagersville, Ontario, Canada (Matalon, 1990). Nearly 35 million scrap tires each year are generated in Canada, and only some (fewer than half) are recycled (Takallou, 2015). The rest goes into landfills or scrap piles like Hagersville's; thus, causing a huge risk of fire. Burning tires are very toxic. Their primary constituents, rubber, and petroleum produce an oily sludge, which can contaminate soil and groundwater, and dense smoke emitted can damage lungs. Moreover, the cost of the fire was calculated in the millions with regards to the scenario in Hagersville (Matalon, 1990). This incident awakened Canadian provinces and the worldwide outlook of approaches towards scrap tire management. Different alternatives for waste tire management apart from landfill disposal includes retreading, reclaiming, incineration, and grinding (Laresgoiti *et al.,* 2004). However, all the techniques have several limitations such as a) Retreading –It is a re-manufacturing process for tires. It reuses less severely worn-off parts of old tires. However, it harms vehicle stability and might lead to accidents (Schnecko, 1998); b) Reclaiming -Due to network breaking, rubbers from waste tires are reduced to low molecular weight fragments which

can be mixed with virgin rubber. This process is labor-intensive with low-profit margins (Bockstal *et al.,* 2019); c) Incineration –Burning of scrap tires involves a lot of pollution by emission of – SO_X and NO_X.

Among all the above, pyrolysis of scrap tires is the most promising route to convert this waste feedstock into valuable products such as pyrolytic oil and carbon black. However, the pyrolytic oil obtained cannot be used as a drop-in fuel. Due to population explosion ("Current World Population", 2021) and subsequent industrialization, our dependence on crude oil and its derivatives such as heavy fuel oils will continue to dominate the global energy mix, though low-grade alternative fuels options are being explored. Crucial environmental concerns include pollution, global warming, and climate change due to poor air quality resulting from the combustion of these oils, and due to high emission levels of sulfur oxides (SO_X) and nitrogen oxides (NO_X). The removal of sulfur-containing compounds is a central requirement to the oil refineries for not only the production of clean fuel oils but also to meet the new standards of sulfur content (10-15 ppm) as per the recommendations of the USEPA (the United States Environmental Protection Agency) for transportation fuel (Hossain *et al.,* 2019). Moreover, sulfur derivatives corrode the combustion engine parts and also poison the catalyst used in the catalytic converter (Bazyari et al. 2016). Also, the global allowable sulfur levels mandate by the International Maritime Organization (IMO: 2020) to be reduced from a cap of 3.5 wt% to 0.5 wt% by January 2020 ("IMO 2020", 2019). With the drastic drop, high sulfur fuel oil (HSFO) prices are expected to drop sharply as most ships and electricity generation companies (relying on crude oils for power generation) switch to burning cleaner, distillate-based bunker fuel blends, and heavy fuel oil. With the high sulfur contents (> 4 wt%) in bitumen, bunker fuel blends, and heavy fuel oils, the common practice of refineries is to typically resort to hydrotreating to remove the refractory organosulfur from these oils via processes known as hydrodesulfurization (HDS). Hydrodesulfurization is the current commercial desulfurization process, which is typically used in petroleum refineries around the world. It can be used to remove sulfur compounds from pyrolytic oil, but it is a hydrogen demanding process. As hydrogen supply is necessary even for smaller amounts of feedstocks, HDS may not be a viable option. Therefore, the sulfur removal processes, which do not use hydrogen such as oxidative desulfurization can be explored for the removal of sulfur species from the oils.

In this research, oxidative desulfurization (ODS) is explored for the removal of organosulfur compounds from tire pyrolysis oil under mild process conditions. It is a more dependable and cost-competitive desulfurization process.

1.2 Knowledge Gaps

Based on the detailed literature review done in Chapter 2, the following knowledge gaps were identified.

a) Research on the removal of sulfur from tire pyrolysis oil through oxidative desulfurization is limited in the literature. Moreover, utilization and process optimization (Temperature ℃, Oxidant/ sulfur (molar ratio), amount of catalyst in oil (wt%)) of Ti-incorporated mesoporous alumina and Ti-incorporated mesoporous TUD-1 have not been extensively reported in the literature for the oxidative desulfurization of tire pyrolysis oil.

b) Sulfur removal by solvent extraction, kinetic study, catalyst re-generability, and reusability have not been performed in detail for oxidative desulfurization of tire pyrolysis oil for these catalysts.

1.3 Hypotheses

a) The incorporation of Ti during the synthesis of mesoporous alumina and TUD-1 and impregnation of molybdenum will have a positive impact on their acidity. In addition, Ti-incorporation will enhance the formation of the titania-peroxo complex which will increase the active sites for sulfur removal, and thus enhance the oxidative desulfurization reaction. During the oxidative desulfurization reaction, optimum process conditions (Temperature ℃, Oxidant/ sulfur (molar ratio), Catalyst/ Oil (wt%)) exist whereby the conversion of sulfur species in the tire pyrolysis oil to their corresponding sulfones will enhance the removal of sulfur species from tire pyrolysis oil.

b) Sulfur removal by solvent extraction, oxidative desulfurization kinetic studies, and catalyst regenerability will help ascertain the durability of the prepared catalyst for the oxidative desulfurization of tire pyrolysis oil application.

1.4 Research Objectives

The overall research objective is to remove sulfur from tire pyrolysis oil through oxidative desulfurization by preparing, characterizing, and applying catalytic material to produce transportation fuel.

Sub objectives:

a) Preparation, optimization, and characterization of heteropolyacid loaded catalysts, Ti incorporated mesoporous material (Al_2O_3 and TUD-1) with different (Ti/Al and Ti/Si) ratios, with Mo (20 wt%) and their subsequent screening tests to optimize process parameters for oxidative desulfurization reaction using tire pyrolysis oil.

b) Oxidative desulfurization kinetic study, sulfur removal by solvent extraction, catalyst regenerability, and reusability evaluation using the optimized catalyst.

Chapter 2: Literature Review

This chapter elaborates on the literature study correlated to this research. Pyrolysis of scrap tires to tire pyrolysis oil presents immense incentives. However, upgrading of tire pyrolysis oil needs to be done to meet the environmental standards. Among many different upgrading techniques, oxidative desulfurization seems most promising. However, its success rests on the optimum catalyst and process conditions that can effectively remove sulfur and nitrogen from tire pyrolysis oil.

2.1 Scrap tire pyrolysis

The conversion of wastes to energy plays a pertinent role in the generation of alternative resources to supplement dwindling conventional resources. Typically, at the end of their lives, waste tires are discarded into landfills where they pose health and fire hazards due to their non-biodegradable nature. Besides, the disposal of scrap tires takes enormous dumping space and hosts potential disease-bearing vectors (Bockstal *et al.,* 2019).

Rubber is a major component of tires. The elemental composition (wt%) of tires is shown in Table 2.1(Juma *et al.,* 2007)(Ahmad *et al.,* 2016)(Puy *et al.,* 2013). Sulfur is also considered an important component of tire composition as it acts as a cross-linking agent. Mechanical strength to tires is given by this cross-linked sulfur bonding during the vulcanization process. Due to this cross-linking agent, reuse and recycling of used tires become difficult as they form SOx (Ahmad *et al.,* 2016). That notwithstanding, waste or scrap tires can be utilized as excellent feedstocks for fuel production as their calorific value is comparable to that of diesel(42-46 MJ/kg) and crude oil(42-47 MJ/Kg) (Schnecko, 1998)(Bunthid *et al.,* 2010). The heating value of an average size passenger tire is between 13000-15000 Btu/lb, which is comparable to coal (Bazyari *et al.,* 2016)("Tire Derived Fuel", 2020).

Pyrolysis of scrap tires is an endothermic process in which low molecular weight products (oil, gas, and char) are obtained by thermal decomposition of organic materials (mainly rubber polymers) in the presence of high heat (> 400°C) and an oxygen-free atmosphere (Quek *et al.,* 2013)(Bunthid *et al.,* 2010).

Table 2. 1 Elemental composition (wt.%) of waste tires

Proximate Analysis		Ultimate Analysis	
Volatile organics	~ 60.0	C	~80.0
Fixed carbon	~ 30.0	H	~7.0
Ash	~10.0	N	~0.4
Moisture	~ 1.2	S	~1.4

Pyrolysis of 100 wt% of scrap tire input yields 55 wt% of pyrolytic oil, 34 wt% of solid char, 10 wt% of gases, 1 wt% of moisture (Islam *et al.,* 2016). There are many variations in the conditions of waste tire pyrolysis with different optimal conditions to produce oil. The common parameters that researchers vary are heating rate, pressure, gas flow rate, tire particle size, and pyrolysis temperature (Quek *et al.,* 2013). The disintegration of the rubber polymers into smaller molecules occurs in-situ in the reactor. Pyrolysis of scrap tires presents immense incentives from environmental protection and economic standpoints. In this regard, waste tires are converted into useful products for heating and electricity generation purposes. This technology employs scrap tires as the principal feedstock to generate pyrolytic oils (which can be upgraded into high-quality drop-in liquid transportation fuels), valuable gases (CO, H_2, CO_2, etc.), and solid (carbon black) products (Ahmad *et al.,* 2016). The molecules which are too small to condense remain as a gas and can subsequently be burned as fuel. The mineral constituent of the tire is removed as a solid char. The char consists of recovered carbon black and pyrolysis char. Carbon black contains a high level of impurities (ash~ 10-15%) that harm its reinforcing properties if it is used in the new tire production process (Bunthid *et al.,* 2010). However, it can be used as a raw material in the rubber, or plastic manufacturing industry which can lead to the reduction of CO_2 emission as there is no new carbon black production (Bunthid *et al.,* 2010). The process has been explained in Figure 2.1.

Pyrolysis of waste tires is an emerging technology, which is both intriguing and a challenging field of research. The structure of pyrolytic oil acquired from scrap tires has been demonstrated to be intricate comprising both short and long carbon chains and single and multiple ring structures. The quality of tire pyrolytic oil to be used as a fuel depends upon two parameters which are energy yield (Heatvalue(MJ/kg) × Oilyield(%)) and sulfur content (%) (Quek *et al.,* 2013). The fuel-grade oil obtained from the pyrolysis of waste tires contains C_6 to C_{24} hydrocarbons with a high

calorific value of around 42 MJ/kg and therefore can be used in many industrial applications like cement kilns, thermal power stations, industrial boilers, and as a transportation fuel (Bunthid *et al*., 2010).
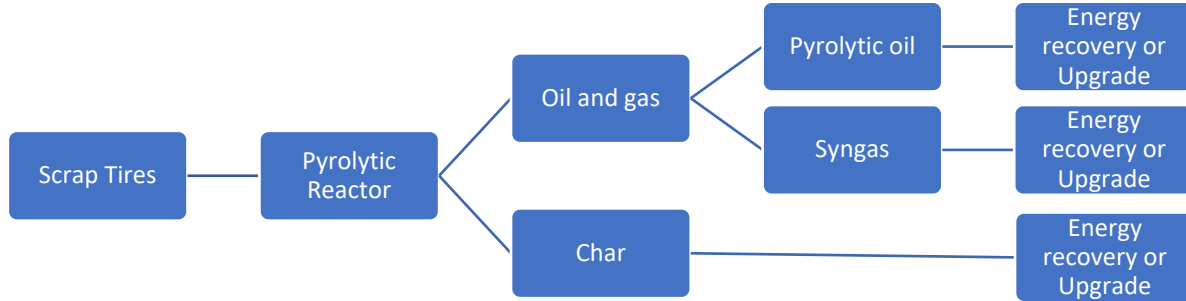
Figure 2. 1 Schematic of scrap tire pyrolysis process

Elemental analysis of tire pyrolysis oil of automotive tires shows that they contain around 85.54% C, 11.28% H, 1.92% O, 0.84% S, and 0.42% N components (Mastral *et al.,* 2000). The characteristics of virgin tire pyrolysis oil are mentioned in Table 2.2 (Islam *et al.,* 2016). Tire pyrolysis oil cannot be used directly as drop-in fuel as it is quite much viscous than regular transportation fuel such as diesel oil (2 cSt at 40°C). However, the main obstacle for using the tire pyrolysis oil directly is the presence of sulfur in concentrations ranging from 0.5 to 3 wt%, which varies with the technology adopted for the extraction of virgin tire pyrolysis oil (Quek *et al.,* 2013).

Table 2. 2 Properties of tire pyrolysis oil

Property	Virgin tire pyrolysis oil
Density at 15°C (kg/L)	0.96
Kinematic Viscosity at 40°C (cSt)	16.39
Flash Point (°C)	50
Pour point (°C)	-3
Gross Calorific Value (MJ/kg)	42

2.2 Classification of pyrolysis processes

The pyrolysis process is classified into many types depending on the operating conditions like temperature, residence time, and heating rate. The main types of pyrolysis are slow pyrolysis and fast/ flash pyrolysis. However, pyrolysis can also be divided based on environmental conditions used like, vacuum pyrolysis, catalytic pyrolysis, steam pyrolysis, and oxidative pyrolysis (Puy *et al.,* 2013). Some of the major types are explained below in detail.

Slow pyrolysis: Fixed bed reactors are typically used to perform slow pyrolysis in a batch process characterized by low temperature and low heating rates with long solid and vapor residence times (minutes to hours) (Alsaleh *et al.,* 2014). Long residence times result in more secondary dissociation of primary products, thus yielding to the formation of more coke and tar and, also thermally stable products. This process is also known as the carbonization process as char is the main product in this process (Puy *et al.,* 2013).

Fast pyrolysis: Fast pyrolysis is usually performed in a fluidized-bed reactor at 500°C – 600°C (Islam *et al.,* 2016). In this process dried small particles of feedstocks are thermally decomposed at heating rates over 300°C/s and vapor residence times of milliseconds to seconds. Fast pyrolysis is known as an effective route to produce high calorific value liquid fuel as it allows condensation of volatiles before further breaking down of high molecular weight compounds into gases.

Catalytic pyrolysis: Catalytic pyrolysis involves using heterogeneous catalysts to increase the yield of pyrolytic oil or change the properties of pyrolytic oil. A wide variety of catalyst materials including zeolites could be used in a rotary kiln or fluidized-bed reactor for pyrolysis (Williams *et al.,* 2002) (Puy *et al.,* 2013). In the case of the tire pyrolysis process, it was reported that the catalyst to tire ratio of 0.1 led to a rise of 8.5 wt% of tire pyrolysis oil yield in comparison to non-catalytic pyrolysis reaction (Puy *et al.,* 2013). Though catalytic pyrolysis is preferred over thermal cracking as it is faster and requires lower temperatures, recovery of the catalyst is difficult after use. Further, the catalyst needs to be regenerated often due to the formation of coke and the poisonous effects of impurities present in the waste tires.

2.3 Upgrading of tire pyrolysis oil

Upgradation of tire pyrolysis oil needs to be done to meet the environmental standards as discussed in chapter 1. For the removal of sulfur, several methods, such as hydrodesulfurization (HDS), adsorptive desulfurization, extractive distillation, supercritical water-based desulfurization, bio desulfurization (BDS), oxidative desulfurization (ODS) can be used but most of these methods are in the development stage (Hossain *et al.,* 2019). However, oxidative desulfurization has shown the most potential among the existing techniques due to its mild operational conditions and higher selectivity than HDS in the removal of aromatic sulfur compounds (Hossain *et al.,* 2019). Table 2.3 presents a summary of possible desulfurization methods for oil upgrading.

At present, the conventional HDS process is commonly employed for most refineries. Hydro desulfurization reactions are carried out in the presence of transition metallic (Ni, Co, and Mo) catalysts at high temperatures (up to 400 °C) and pressure (up to 100 atm) using hydrogen gas. Ni/Co-promoted Mo, W-based bi-, and tri-metallic catalysts have been considered very promising for the development of modified ULSD catalysts (Low *et al.,* 2019). Alumina support, for instance, can be optimized by new additives and incorporation of second support to increase the catalyst stability and selectivity (Jorge *et al.,* 2019).

For heavy gas oil, the sulfur content can be lowered to typically 2200 ppm from 40,000 ppm approximately upon hydrotreatment (Badoga *et al.,* 2018). To lower the sulfur content from 2200 ppm to less than 15 ppm requires higher pressures, hydrogen flow rates and temperatures for the removal of sulfur from refractory molecules such as alkyl substituted dibenzothiophenes (DBT). However, increasing the temperature and pressure leads to the cracking of oil (Badoga *et al.,* 2018). Cracking breaks down large molecules (which is good). Further cracking produces smaller molecules, mostly gas, which is not a favored route. Furthermore, high-pressure processes lead to huge capital investment. That notwithstanding, oxidative desulfurization has gained attention in the desulfurization of fuel oil due to its operation in mild conditions (low pressure and temperature) and relatively low operating costs. Furthermore, the extracted sulfur compounds and the solvent used in the process can be recycled (Houda *et al.,* 2018).

Table 2. 3 A summary of different desulfurization techniques

No.	Desulfurization Technique	Principle	Advantages	Disadvantages	References
1	Hydrodesulfurization	Catalytic Reactions	Highly efficient	High Reaction conditions and operational cost	(Hossain *et al.,* 2019)
2	Oxidative desulfurization	Catalytic reaction and subsequent extraction.	Mild operating conditions, low operating costs	Not commercially accepted due to low selectivity of sulfides in the feedstock, recovery, and catalysts separation	(Hossain *et al.,* 2019)(Farshi, 2015)
3	Extractive Distillation	Solubility	Easier industrial application, hydrogen is not required, adequate and mild process conditions	Desulfurization of only light petroleum cuts, High energy consumption due to multistage desulfurization	(Zeelani *et al.,* 2016)
4	Adsorptive Desulfurization	Absorbability, Selectivity	Simple operating conditions, cost-effective process	The low percentage of sulfur removal along with the removal of aromatic compounds from the feed.	(Zeelani *et al.,* 2016)
5	Bio Desulfurization	Microbial action	Lower capital and operational cost	Difficulty in storage, shipment, and use of microorganisms in an industrial environment and proper management of sanitary handling	(Javadli *et al.,* 2012)
6	Supercritical Water-based Desulfurization	Solubility	Dilution, precipitation of sulfur-rich species, and hydrogen production	Not applicable for aromatic sulfur compounds, can be used in combination with HDS	(Javadli *et al.,* 2012)

During the oxidative desulfurization reaction, the sulfur-containing compounds present in the heavy fuel oil are converted to their corresponding sulfones or sulfoxides in the presence of oxidative agents such as O_2, H_2O_2, etc., and a catalyst such as heteropolyacid, CH_3COOH, HCOOH, etc. Subsequently, the oxidized sulfur compounds are separated from reaction mixtures by filtration followed by adsorption or liquid-liquid extraction technique as shown in Figure 2.2 (Hossain *et al.,* 2019).
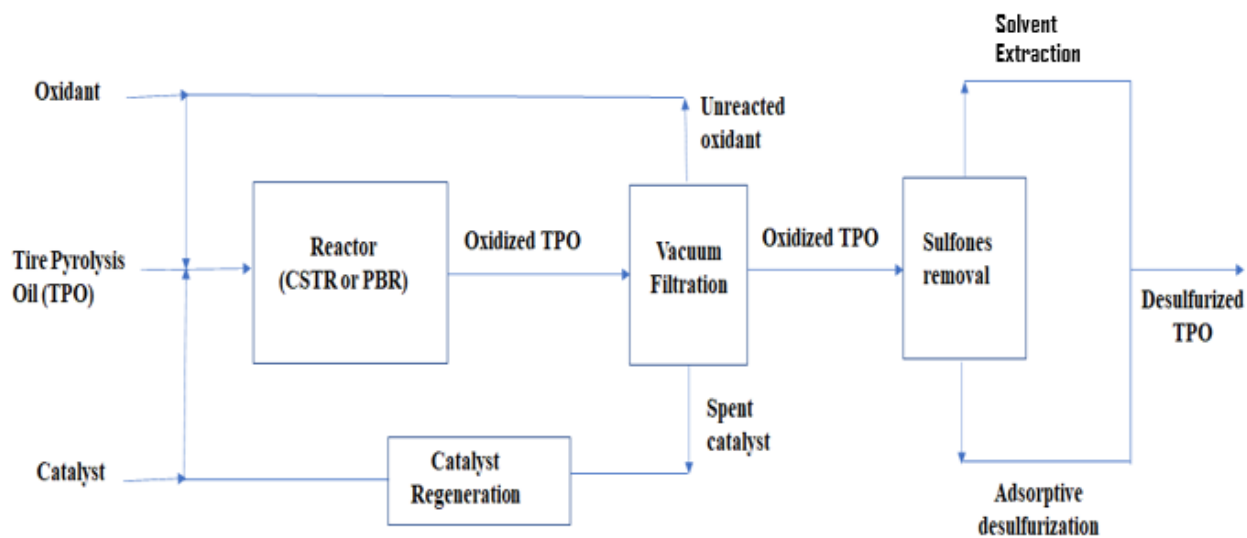
Figure 2. 2 Schematic of oxidative desulfurization of tire pyrolysis oil

2.4 Reactivity of sulfur compounds

One of the advantages of oxidative desulfurization over hydrodesulfurization is the higher reactivity of refractory sulfur compounds (generally present in fuel oil such as heavy fuel oil, tire pyrolysis oil, etc.) as discussed earlier. The reactivity order followed by oxidative desulfurization is 4,6-dimethyldibenzothiophene (4,6-DMDBT) > Dibenzothiophene (DBT) > Thiophene (Hossain *et al.,* 2019).The reactivity of sulfur-containing compounds rises due to the electron-donating property of alkyl side chains hence enhancing the electrophilic attack on the oxygen by the sulfur atom due to an increase of corresponding electron density (Houda *et al.,* 2018). In addition to the increase in electron density on the sulfur atom and steric hindrance caused by alkyl substituents, inductive effect (an effect regarding the transmission of unequal sharing of the bonding electron through a chain of atoms in a molecule, leading to a permanent dipole in a bond) has a positive effect on the reaction rate (Krivtsov *et al.,* 2014).

Unoxidized sulfur has higher bond dissociation energy as compared to oxidized sulfur for instance CH_3S-CH_3 has a bond dissociation energy of 320 kJ mol^{-1} while at the same time its corresponding oxidized sulfur compounds, $CH_3(SO)-CH_3$ and $CH_3(SO_2)-CH_3$, have bond dissociation energies 230 kJ mol^{-1} and 280 kJ mol^{-1}(Serefentse *et al.,* 2019).

2.5 Oxidative desulfurization system

Oxidative desulfurization is a two-step process that includes oxidation reaction, and solvent/adsorbent extraction (Farshi, 2015) (Hossain *et al.,* 2019)as shown in Figure 2.3.
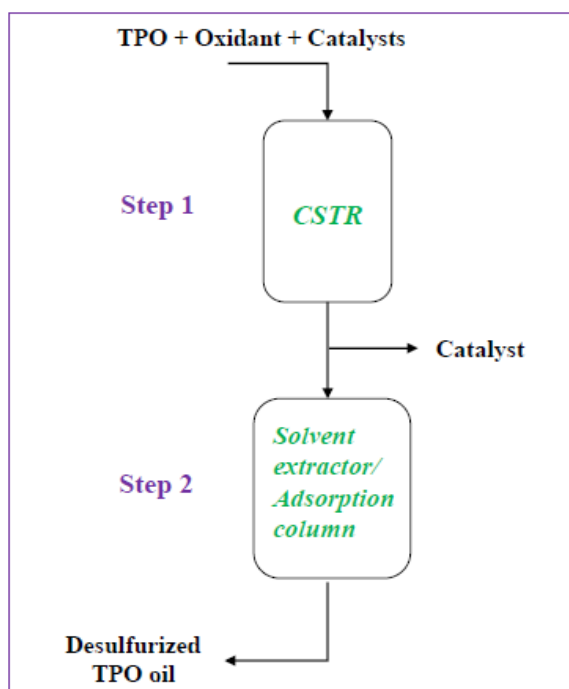
Figure 2. 3 Schematic representation of sulfur removal in the oxidative desulfurization process

On the addition of an oxidant, bivalent sulfur is oxidized to hexavalent sulfone; it comprises of the addition of two oxygen atoms to the sulfur without any breakage of carbon-sulfur bonds with the formation of sulfoxide as an intermediate as shown in Figure 2.4 (Houda *et al.,* 2018). In the next step, sulfoxides, and sulfones, polar in nature, are removed by extraction or adsorption by extracting solvent. The chemical and physical properties of oxidized sulfur compounds are considerably different from hydrocarbons of crude oil. Hence, they can be easily removed by

various separation techniques like adsorption or extraction. As given in Table 2.4, homogeneous and heterogeneous catalysts like ChFeCl4 (Fenton like hybrid catalysts), TS-1 (Titanium silicate), and HZSM-5 (aluminosilicate zeolite) were applied for oxidative desulfurization at atmospheric pressure.
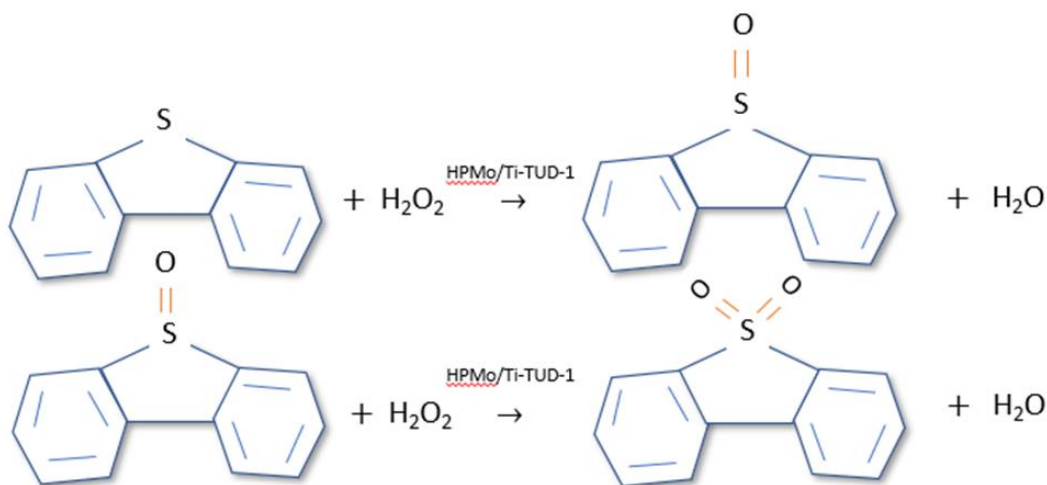
Figure 2. 4 Oxidation reaction pathway of sulfur compounds with HPMo/ Ti-TUD-1 as catalyst and H_2O_2 as oxidant

Desulfurization through ODS was proven with model and simulated petroleum feedstocks using oxidants such as hydrogen peroxide, tert-butyl hydroperoxide (TBHP), and cumene peroxide (Estephane *et al.,* 2018).

Tire pyrolysis oil was desulfurized by the ODS technique to use as heating oil by Ahmad *et al.,* 2016. They reported the best desulfurization activity with hydrogen peroxide–acetic acid mixture. Hydrogen peroxide–formic acid mixture was also found to be effective for ODS of tire pyrolytic oil (Doğan *et al.,* 2012). Al-Lal et al. 2015 desulfurized waste tire pyrolysis oil that contained 8700 ppm of sulfur using formic acid (85 wt.%) and hydrogen peroxide (50 wt.%) combination under ultrasound at 70 °C for 30 min. A desulfurization rate of 53% was reported after three successive extractions of oxidized oil with methanol. The naphtha fraction of tire pyrolysis oil was desulfurized with a mixture of pyrolytic char, formic acid, and hydrogen peroxide by Bunthid *et*

al., 2010. They observed 70% of desulfurization due to simultaneous adsorption and oxidation of sulfur compounds on the surface of the pyrolysis char.

Table 2. 4 Oxidative desulfurization of petroleum fuels and model sulfur compounds

Source of sulfur	Catalyst and oxidant	Reaction conditions	Sulfur removal (wt.%)	References
Gasoline	ChFeCl$_4$ and H$_2$O$_2$	T= 30 °C, t =30 min	97.0	(Jiang *et al.,* 2014)
Diesel/DBT	TiO$_2$ and H$_2$O$_2$	T= 40 °C, t =90 min	99.1	(Zheng *et al.,* 2015)
DBT	Mesoporous TS-1 and TBHP	T= 80 °C, t = 180 min	96.0	(Afzalinia *et al.,* 2017)
Model oil (BT, Thiophene, DBT)	Copper phthalocyanine molecular sieve/HZSM-5 and O$_2$	T=60 °C, t= 180 min	Thiophene= 93.0 BT= 91.0 DBT= 87.0	(Wang *et al.,* 2015)
Gas oil	HCOOH and H$_2$O$_2$	T=50 °C, t=46 min	96.2	(Q. Tang *et al.,* 2013)
Crude oil	CH$_3$COOH and H$_2$O$_2$	T=90 °C, t= 15 min	78.7	(Mohammed *et al.,* 2012)

2.6 Non-catalytic system

Study on the non-catalytic process, direct chemical oxidation of sulfur compounds, is scarce in the literature. Autoxidation reaction using atmospheric oxygen was conducted with tar sand bitumen comprising sulfur (5.2%) (Javadli *et al.,* 2012). Reactions were carried out at various temperatures below 200°C. On rising the temperature above 175°C, the bitumen hardening was noticed due to an increase in viscosity. Researchers concluded that it might be due to the free radical mechanism caused by the complex nature of bitumen. The optimized conditions noted were 145°C for 3 h to

obtain the desulfurization rate of 46% (Javadli *et al.,* 2012). The main drawback shown by different studies for non-catalytic techniques performed using selective oxidizing agents like air, ozone (Kazakov *et al.,* 2016), or nitrogen oxides (Houda *et al.,* 2018) is the emission of sulfur as SO_2 which is the main cause of environmental pollution.

Oxidative desulfurization by liquid oxidants like nitric acid, potassium permanganate, and sodium hypochlorite (Houda *et al.,* 2018), without the use of catalysts, has also been reported in the literature. Nitric acid was used as an oxidant (100 ml) for the conversion of sulfur, present in coal (20 g), to sulfate and captured in the ash, avoiding the release of SO_2 to the environment. The desulfurization rate of 35 % was achieved at ambient temperature (Gürü, 2007). A catalytic oxidation system is considered advantageous over a non-catalytic system due to its simple oxidation process, mild operating conditions, and better efficiency (Houda *et al.,* 2018).

2.7 Catalytic system

The oxidative desulfurization catalytic system is categorized into two forms: Homogenous and Heterogeneous catalytic systems.

2.7.1 Homogeneous catalytic system

The high-efficiency rate caused by the one-phase catalyst system enhanced the wide use of homogeneous catalysis in the oxidative desulfurization of high sulfur fuel oil.

A system of acetic acid as the catalyst and hydrogen peroxide as the oxidant was used to desulfurize the heavy oil (Farshi, 2015). A glass batch reactor was used to conduct the experiment. The lowering of sulfur from 2.75 wt% to 1.14 wt% was achieved under the following optimized reaction conditions: reaction time of 90 min, reaction temperature of 60°C with a stirring rate of 750 rpm, and oxidant to sulfur molar ratio equal 5 (Farshi, 2015). Another model using formic acid as a catalyst and hydrogen peroxide as an oxidant was also studied. Acetonitrile was used as a solvent for extraction. 100 % sulfur removal efficiency was achieved under the optimal reaction conditions of catalyst to sulfur molar ratio of 222:1, oxidant to sulfur ratio as 2:1, reaction temperature as 65°C, and reaction time of 56 min (Haghighat *et al.,* 2013). A major development studied in homogeneous catalyst system was the introduction of peroxometallates as catalysts. Peroxometallates are salts of transition metals that form peroxycomplexes, improving catalytic

efficiency when used in the oxidative desulfurization process (Houda *et al.,* 2018). However, the liquid acid-peroxide oxidation system has certain disadvantages such as separation problems due to the use of oil-soluble organic acid as a catalyst and the non-renewability of catalysts (Hossain *et al.,* 2019).

2.7.2 Heterogeneous catalytic system

Heterogeneous catalysis has advantages like easy product generation, eco-compatibility, and catalyst separation which could not be fully achieved by a homogeneous catalyst system (Houda *et al.,* 2018).

For the oxidative desulfurization of high sulfur content (>0.5 wt% S) fractions, a heterogeneous catalyst system comprises of one active phase, mainly based on transition metals, dispersed on the support to achieve a larger surface area. Molybdenum, vanadium, and tungsten are commonly used transition metals as reported in the literature. Meanwhile, alumina, silica, and zeolites are used as supports in several studies (Houda *et al.,* 2018).

A functional polymer-based catalyst was studied for the oxidative desulfurization of aromatic fraction of heavy sulfur fuel oil using tert-butyl hydroperoxide. Nanofibers were used for the adsorption of sulfones obtained. The sulfur removal of 0.89% was achieved from 1.8% with an oxidant to sulfur ratio equal to 20 (Ogunlaja *et al.,* 2017).

The incorporation of several heteroatoms such as Al, Ti, and Zr on SBA-15 was studied. Researchers found a decrease in surface area and pore volume of the support due to significant segregation of metal oxides on the surface, on heteroatom incorporation beyond 20 wt%, hence, causing a decrease in catalytic activity due to a decrease in the dispersion of active sites. The addition of 5-10 wt% titanium led to a rise in catalyst activity rather than Zr incorporation (Rivoira *et al.,* 2016).

There are several studies reported on ODS of tire pyrolysis oil such as when 53% of desulfurization was obtained by using H_2O_2- formic acid system as an oxidant-catalyst, followed by liquid-liquid extraction where methanol was used as a solvent (Al-Lal *et al.,* 2015). However, if distilled water was used for extraction desulfurization rate surged to 64% (Zhang *et al.,* 2020). According to Zhang et al. 40 % of sulfur was itself removed from ODS reaction and a maximum of 66% was removed by solvent extraction. Furthermore, the solvent fraction was further treated by Al_2O_3 adsorption thus leading to a sulfur removal efficiency of 84% (Zhang *et al.,* 2020).

Titanium incorporation

It has been found that the incorporation of titanium in supports can promote oxidation due to its Lewis acid character (Fraile *et al.,* 2016; Shen *et al.,* 2016). The site for nucleophilic attack by the oxidant is provided by electron-deficient in titania that leads to the formation of the peroxo-titania complex. The complex formed activated the oxidation of sulfur compounds. Thus, oxidative desulfurization activity is increased by the incorporation of titanium (Shen *et al.,* 2016).

As per the increase in efficiency of titanium-based catalysts in oxidation reactions; their applications in oxidative desulfurization have also been studied by researchers. TS-1 zeolite, Ti–HMS silica, Ti-MCM48, and TiO_2 nanotubes have been used in the removal of sulfur compounds (Fraile *et al.,* 2016). Typical catalytic supports such as alumina, silica, titania show low oxidative desulfurization activity in the removal of dibenzothiophene derivatives (Rivoira *et al.,* 2016). Titanium incorporated supports such as mesoporous Ti- modified SBA-15 and titanium oxide nanotubes have been used as alternatives for the oxidative desulfurization process due to the large surface area. Titanium oxide nanotubes have gained attention due to several advantages like economical, high specific area, and feasibility for the production in large quantities (Cedeño *et al.,* 2011).

Mesoporous supports

Crystalline titanium silicate-1 is an efficient catalyst for the oxidation of thiophene. However, due to its small pore size, it exhibited very low catalytic efficiency towards benzothiophene and dibenzothiophene. Hence, many efforts were devoted to making crystalline Ti incorporated silica with larger pores (Ti-SBA-15, Ti-HMS, Ti-SBA-16, etc) but they suffered from the lower catalytic activity and instability (Bazyari *et al.,* 2016). A similar kind of trend was observed with zeolites-based catalysts. Supports with mesoporous channel structure with various advantages like high surface areas, large pore volumes, lightweight, and thermal stability has aroused the interest of several researchers to use them for the deep desulfurization of fuel oils (Ding *et al.,* 2015; Vedachalam *et al.,* 2020). Mesoporous titanium silicate-1 (TS-1) using a hybrid SiO_2-TiO_2 xerogel has been studied by Yang *et al.,* 2012 for the removal of sulfur compounds from model oil dissolved in n-octane. H_2O_2/ acetic acid was used as an oxidant system which led to the oxidation of sulfur refractory compounds such as benzothiophene, dibenzothiophene, and 4, 6 dimethyl

dibenzothiophene. The reaction was performed for mesoporous TS-1 and conventional TS-1. The reaction took place in a 100 ml batch reactor with 300 rpm at 80°C. The sulfur compounds conversion was observed to be higher using the former that was 98% while for the latter was 5.6% (Yang *et al.,* 2012).

Mesoporous Alumina

Mesoporous alumina as catalyst support is prioritized over other supports due to its stable pore structures, easy preparation, and low cost (Jin *et al.,* 2017). By changing the synthesis parameters, mesoporous alumina with adjustable pore size can be produced (Čejka, 2003). Mesoporous alumina as support has shown a prominent desulfurization rate with DBT and TBHP/H_2O_2 as an oxidant (D. Wang *et al.,* 2003; Jin *et al.,* 2017).

Mesoporous TUD-1

Mesoporous silica has shown efficient desulfurization rates with large 4,6 DMBDT and DBT molecules(Cho *et al.,* 2014; Cruz *et al.,* 2019). Mesoporous TUD-1 is a mesoporous silicate very straightforward to prepare. It has a sponge-like three-dimensional and irregular structure. Its fast diffusion property makes it ideal for catalyst development (Telalović *et al.,* 2010). Mesoporous TUD-1 support has been considered a valuable catalyst carrier due to its tunable textural properties, high stability, and the possibility of the substitution of several metals in its framework (Telalović *et al.,* 2010). Moreover, TUD-1 uses triethanolamine as a template, which is much economical thus reducing the preparation cost of the oxidative desulfurization catalyst (Tang *et al.,* 2013). 20 HPW-TUD-1 resulted in a desulfurization rate of 98.1% at 60°C optimal reaction temperature (Tang *et al.,* 2013).

2.8 Influence of process parameters on oxidative desulfurization

There are certain major parameters such as reaction temperature, reaction time, oxidant to sulfur ratio, stirring conditions, etc. that influence the oxidative desulfurization process and its possibility of scaling up to industrial scale. Some of the major influencing factors are discussed below in detail.

2.8.1 Reaction temperature

The reaction temperature is a major parameter that affects the oxidative desulfurization reaction. Oxidative desulfurization reaction is exothermic. Several temperature ranges have been tested in the literature. Oxidation reactions in the catalytic system are generally performed in the temperature range of 35-90℃. Oxidative desulfurization of petroleum feed was studied at 35°C. Hydrogen peroxide and formic acid oxidant system was used with an oxidant to an acid molar ratio of 3:4 for the desulfurization of high sulfur diesel straight run gas oil. Oxidation followed by adsorption by silica gel led to removal of sulfur from 1.19 wt % to 0.05 wt% with the reaction time of 8 h (Krivtsov, 2014). It was noticed from the literature that increase in temperature from 35℃ to 90℃ increased the sulfur removal, however, the increase in temperature beyond 90℃ had a negative impact as it might lead to oxidant degradation and oxidation of other useful compounds and result in the formation of asphaltenes and resins (Toteva *et al.,* 2009). Along with the rise in oxidation rate by increasing the reaction temperature, the acceleration of desorbed oxidized sulfur species from the catalyst's active sites also increases. This could be the reason for the decrease in desulfurization rate with rising temperature beyond optimum value (Wei *et al.,* 2016).

2.8.2 Reaction time

Reaction time is a critical parameter in every existing reaction. As per the literature, reaction time for the catalytic system was mostly studied between 1-10 hours (Houda *et al.,* 2018). It was believed that an increase in reaction time may lead to a rise in the sulfur reduction rate. However, the researchers noticed a decrease in sulfones concentration at a reaction time of more than 2 h, possibly due to oxidation of sulfones to sulfates (Toteva *et al.,* 2009).

2.8.3 Oxidant to sulfur ratio

The amount of oxidant used is also considered as one of the major factors in determining the desulfurization rate. Several experiments were conducted with different oxidant to sulfur ratios to achieve the highest amount of conversion of sulfur to sulfones. An increase in the amount of oxidant increases the desulfurization activity in every possible way. Abubakar *et al.,* 2016 studied the desulfurization of crude oil with different oxidant to sulfur ratios ranging from 1:1 to 5:1. The crude oil contained 1.13 wt% sulfur which was reduced to 0.74 wt% sulfur at O/S=1 to 0.43 wt% sulfur at O/S=5 (Abubakar *et al.,* 2016). However, due to economic factors, the best oxidant to the

sulfur ratio found by Abubakar is 2 as they found not much increase in the percentage of sulfur removal with the ratios above 2. But still, in some cases, a valid increase in the amount of oxidant is required depending upon the heavy nature of petroleum fraction feed as they lead to side reactions during oxidation (Houda *et al.,* 2018). A remarkable rise in desulfurization rate was observed with H_2O_2 and DBT until O/S =10:1, with no major rise beyond that ratio was seen while varying it from 2.5:1 to 15:1 (Sengupta *et al.,* 2012).

Apart from all reasons, less quantity of oxidant is always preferred due to environmental and economic factors. Hence, is considered as the need for the researchers to work upon while studying the oxidative desulfurization process.

2.9 Oxidative desulfurization kinetic study

Kinetics is used to determine the reaction mechanism and its pathways. Contact time and adsorbent dosage are usually used to determine the adsorption kinetics of refractory sulfur compounds (Saleh *et al.,* 2016). It was found that as the contact time increased, more sulfur compounds were attached to the adsorbent, and the number of adsorption sites decreased. While the increase in adsorbent dosage led to an increase in external diffusion parameters and lower intraparticle diffusion parameters in the case of alumina (Daniel *et al.,* 2018). Pseudo-first-order, pseudo-second-order, and intraparticle diffusion models are used to analyze sulfur reaction kinetics (Saleh *et al.,* 2016). The equations of all the three kinetic models are given as 2.1, 2.2, and 2.3.

Pseudo-first-order kinetics

The initial stages of the reaction are analyzed by pseudo-first-order kinetics. This model describes a reversible equilibrium on adsorbate and adsorbent (Earvin *et al.,* 2014).

$$\ln (C_0 / C_t) = - k_1 t \qquad (2.1)$$

where C_0 (mg/g) and C_t (mg/g) are the amounts of analyte adsorbed at time zero and time t (min), respectively; and k_1 (min^{-1}) is the rate constant of the pseudo-first-order kinetics model.

Pseudo-second-order kinetics

 The whole adsorption process and overall adsorption capacity are explained by the pseudo-second-order kinetic model. It is based on the assumption that the rate-limiting step is chemisorption (Daniel *et al.,* 2018).

$t/C_t = (1/(k_2 C_0^2)) + (t/C_0)$ (2.2)

Where C_t is the amount of DBT (mg/g) at a time (min) and k_2 (g/(mg min)) is the adsorption rate constant of pseudo-second-order adsorption.

Intraparticle diffusion model

The intraparticle diffusion model is used as a tool to understand the mechanisms and to find rate-controlling steps affecting the reaction kinetics (Saleh *et al.,* 2016).

$C_t = kid\ t^{0.5} + C$ (2.3)

Where C is the intercept (mg/g) which is related to the boundary layer thickness and k_{id} is the slope which represents the intraparticle diffusion rate constant. If the plot of q_t vs $t^{0.5}$ is linear and passes through the origin, then intraparticle diffusion is the sole rate-limiting step. If the plots do not pass through the origin then the intraparticle diffusion is not the only rate-controlling step (Saleh *et al.,* 2016).

There is limited research about the rate of reaction vs. oxidant as in most cases catalytic oxidative desulfurization reaction occurs with an excess of oxidant (H_2O_2, TBHP, or O_2). It is accepted that the reaction kinetic is of the zeroth order on oxidant amounts. It was proved by plotting the reaction rate constant against the concentrations of H_2O_2, and hence obtaining the reaction order of H_2O_2 as zero (Kong *et al.,* 2004). Years of research have shown that the catalytic oxidation reaction of sulfur present in the fuel oils is of the first or pseudo-first order of sulfur compounds (Kong *et al.,* 2004)(Krivtsov *et al.,* 2014). In some cases, the catalytic oxidation reaction is of zeroth-order on the sulfur compound, when fuel oil contains a high concentration of refractory sulfur compounds (Earvin *et al.,* 2016)

2.9.1 Criteria for the elimination of internal and external mass transfer

There are two types of mass transfer diffusion resistance: 1) *external mass transfer-* Diffusion of reactants or products between the bulk fluid and the external surface of the catalyst and, 2) *internal mass transfer-* Diffusion of reactants or products from external pellet surface to interior of the pellet (Fogler, 2004). Mass transfer effect has been studied in literature by comparing two-liquid phase system. A better conversion was obtained at the L-S (Liquid-Solid) phase rather than the L-L-S (Liquid (oil)-Liquid (solvent)-Solid (catalyst)) phase probing the existence of mass transfer limitation in the reaction. So, it is better to obtain kinetic data with a two-phase system (Rivoira *et*

al., 2016). Mass transfer limitations have been encountered for oxidative desulfurization processes, and previous studies determined that the only useful comparison of catalytic activity could be made when the L–L mass transfer effects were eliminated (Dedual *et al.,* 2014). There are several assumptions followed to obtain suitable rate data such as 1. If the reaction performs at high stirring speed diffusion limitations are neglected and, 2. As the catalyst is used repeatedly for several experiments, catalyst deactivation is not coupled to kinetic models (Dhir *et al.,* 2009). The assumptions are explained as follows:

1. Effects of speed of agitation

The study of the degree of agitation is important in a heterogeneous reaction with a solid catalyst to differentiate the mass transfer limited region to obtain kinetic data (Jose *et al.,* 2011). Researchers found that sulfur conversion was not affected at or above 1000 rpm (Jose *et al.,* 2011). Hence, it was assumed that reaction was external mass transfer free and kinetically controlled at or above 1000 rpm. There was another study where external mass transfer limitation was evaluated by changing stirrer speeds from 200-800 rpm to determine the external mass transfer effect (Rivoira *et al.,* 2016). The rate of reaction was found to increase initially with the increase in stirrer speed. However, the rise was insignificant with a further increase of stirrer speed at or above 300 rpm. Hence, indicating the independence of reaction rate on speed (Rivoira *et al.,* 2016).

2. Influence of particle size of the catalyst

The mechanism of sulfur refractory compounds adsorption on catalyst involves several steps. In the first step sulfur compound molecules are migrated from the bulk of the solution to the surface of the catalyst. The second step includes the diffusion of the sulfur compound through the boundary layer to the surface of the adsorbent. In the third step, the adsorption of sulfur occurs at an active site on the surface of the catalyst and the last step is the intra-particle diffusion of sulfur into the interior pores of the adsorbent (Saleh *et al.,* 2016).

The intraparticle mass transfer resistance was studied by the researchers using different particle sizes of catalyst. It was observed that sulfur conversion was almost the same with change in particle size (at similar conditions) due to the insignificant effect of internal diffusion to mass transfer after a particular particle size range (less than or equal to 460 μm)(Jose *et al.,* 2011).

2.10 Catalyst deactivation and reusability

Deactivation of the catalyst is very important from an industrial point of view. In literature, the reusability of the catalyst for the ODS of refractory sulfur compounds has been tested after washing with solvent (such as water, methanol) and after washing followed by calcination in muffle furnace as it was observed that the activity of the calcined sample remains even after multiple recycle compared to a fresh catalyst (Rivoira *et al.,* 2016). Solvent washing is done to remove the oxidized products adsorbed on the catalyst and the regeneration of the catalyst by calcination is done to ensure the complete elimination of organic compounds that could block the catalyst pores. The stability of the material's structure after recycling can be ensured by XRD (X-ray Diffraction) and TEM (Transmission electron microscopy)(Rivoira *et al.,* 2016).

2.11 Summary

Research on ODS of tire pyrolysis oil over heteropolyacid catalysts is limited in the literature. Moreover, catalysts supported on mesoporous Ti-Al$_2$O$_3$ and Ti-TUD-1 have not been studied for the oxidative desulfurization of tire pyrolytic oil. In this study, two different series of heteropoly molybdic acid-loaded catalysts were prepared based on Ti-Al$_2$O$_3$ and Ti-TUD-1 supports. The impact of Ti substitution in both types of supports on ODS was investigated. Efficiencies of various oxidants such as hydrogen peroxide, tert-butyl hydroperoxide, and cumene hydroperoxide were studied for ODS tire pyrolytic oil. ANOVA statistical analysis was carried out with optimal catalyst and oxidant to investigate the significance of process parameters.

Chapter 3: Research methodology

Based on the literature study done in Chapter 2, the experimental work performed for this research is discussed in this chapter. The overview of catalyst preparation, its characterization techniques, and oxidative desulfurization runs have been studied.

3.1 Preparation of supports and catalyst

Catalysts were prepared first by the preparation of the support followed by the impregnation with heteropolyacid with Mo (20 wt%).

3.1.1 Ti-Al$_2$O$_3$ support preparation

The mixed metal oxides alumina support preparation followed the approach adapted from Lesaint *et al.,* 2008 which led to the synthesis of mesoporous alumina support (Lesaint *et al.,* 2008).

In preparation of titanium incorporated alumina support, chemicals used were Pluronic F127 (Sigma Aldrich, Oakville, Canada), aluminum tert-butoxide 97% (C$_{12}$H$_{27}$AlO$_3$) (Acros Organics, Saskatoon, Canada), absolute ethanol (EtOH) (Commercial alcohols, Saskatoon, Canada), and isopropanol (iPrOH) (Fisher Scientific, Ottawa, Canada). F127 provides the framework while aluminum tert-butoxide is used as an aluminum precursor.

The amount of titanium precursor (titanium isopropoxide) used was calculated. An appropriate amount of Pluronic F127 was dissolved in the mixture of ethanol and isopropanol upon proper stirring followed by the addition of aluminum tert-butoxide. Different amounts of titanium isopropoxide (Sigma Aldrich, Oakville, Canada) were added corresponding to different Ti/Al ratios. Then, the calculated quantity of distilled water was added with continuous stirring. In addition to water, the white suspension was converted to gel. After cooling the gel to room temperature, it went through hydrothermal treatment. Then, the material was calcined leading to the formation of a series of titanium incorporated mesoporous Al$_2$O$_3$ supports.

3.1.2 Ti-TUD-1 support preparation

The TUD-1 support synthesis was done by following the steps performed by Badoga *et al.,* 2014 which led to the formation of titanium incorporated mesoporous support.

In preparation of titanium incorporated TUD-1 supports, chemicals used were tetraethyl orthosilicate 98% (Sigma Aldrich, Oakville, Canada), titanium butoxide 99% (Alfa Aesar, Saskatoon, Canada), triethanolamine 99% (Sigma Aldrich, Oakville, Canada), and tetraethylammonium hydroxide 35% (Sigma Aldrich, Oakville, Canada). Triethanolamine was used as a template for mesopores formation, while tetraethyl orthosilicate is used as a silica precursor. Furthermore, tetraethylammonium hydroxide controls the support's active sites. A stepwise mixing of these chemicals is performed followed by hydrothermal treatment and calcination ultimately leading to the synthesis of different TUD-1 supports with Ti/Si ratios.

3.1.3 Preparation of heteropolyacid loaded catalysts

To prepare the catalyst, 20 wt% Mo was impregnated on prepared supports using Heteropolymolybdic acid (HPMo). 12-Molybdophosphoric acid hydrate ($H_3PMo_{12}O_{40}$) (Sigma Aldrich, Oakville, Canada) was used as a precursor for keggin type heteropolyacid. The titanium-incorporated mesoporous Al_2O_3 supports were mixed with an aqueous solution of phosphomolybdic acid, while titanium-incorporated mesoporous TUD-1 supports were mixed with a methanol solution of phosphomolybdic acid followed by drying and calcination.

3.2 Physicochemical characterization of supports and catalysts

3.2.1 X-ray Diffraction (XRD)

XRD is a powerful non-destructive material characterization technique used to collect detailed information on the crystallographic structure of the material. X-rays are ionizing radiations with both electric and magnetic properties and are produced by interactions between the external electron beam and the electrons on the shells of an atom. The working of XRD is by exposing the material to the incident X-rays and then measuring the scattering angles and intensities of the X-rays leaving the material after its interactions. It depends on the constructive interference of the sample to be tested and the monochromatic X-rays (Holder *et al.,* 2019). The schematic of the XRD instrument is shown in Figure 3.1. The crystallographic structure and morphology of prepared catalysts were analyzed using the XRD in this research. To conduct XRD analysis Bruker AXS D8 diffractometer (Bruker Optics Inc, Billerica, USA) was used. XRD analysis was performed in the wide-angle range (2θ = 10 to 90°) with the above-mentioned diffractometer via

radiation source of Cu Kα generated at 40 kV and 40 mA with λ= 0.15406. The scanning of every sample was done at a rate of 3°C per min.
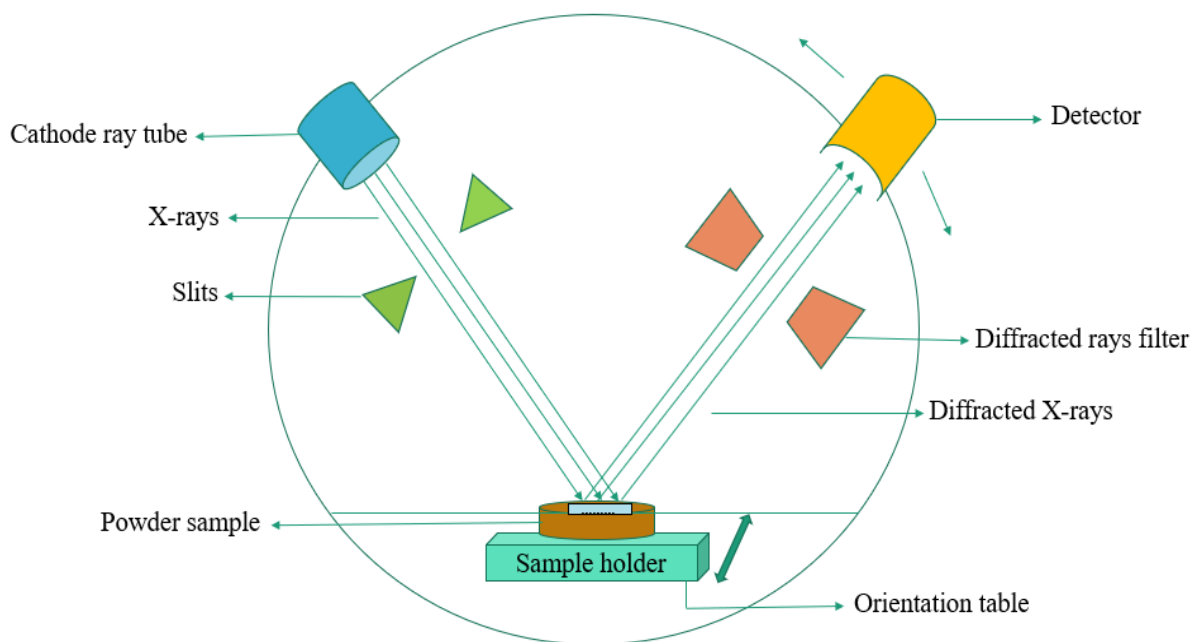
Figure 3. 1 Schematic representation of X-ray Diffraction instrument

3.2.2 N_2 Adsorption Desorption isotherms

The textural properties such as BET surface area, pore-volume, and pore diameter of the supports and catalysts were measured using a Micromeritics ASAP 2020 instrument (Micromeritics Instrument Corporation, Norcross, USA). Before analysis, all the samples were degassed at 200 °C to remove the moisture in the sample. The surface area and textural properties were calculated from adsorption-desorption of nitrogen at -196 °C by the multipoint Brunauer-Emmett-Teller (BET) method. The pore volume was calculated by the amount of N_2 adsorbed at the condition P/P_o=0.95. The pore diameter and pore size distribution were determined using the Barret-Joyner-Halenda (BJH) method.

3.2.3 NH_3-Temperature programmed desorption (NH_3-TPD)

The analysis of the quantity and strength of catalyst acidity was done by carrying out ammonia - TPD in Micromeritics AutoChem 2950 HP Chemisorption Analyzer (Micromeritics Instrument Corporation, Norcross, USA) instrument. In a quartz tube, 40 mg of sample was taken and pre-

treated in the instrument. In a quartz U tube, 40 mg of the sample was loaded and then degassed 300 ℃ under the flow of helium for 30 min. The degassed sample was purged with 15% NH_3 in He at 100 °C.

3.2.4 Fourier Transform Infrared Spectroscopy (FTIR)

FTIR analysis was performed for the confirmation of functional groups present in the supports and catalysts. Bruker Vertex 70 FTIR spectrometer (Bruker Optics Inc, Billerica, USA) instrument was used for operating the analysis.

3.2.5 Pyridine Fourier Transform Infrared Spectroscopy

Fourier transform infrared spectroscopy with pyridine (Pyridine FTIR) as a probe molecule was used for differentiating Lewis and Brønsted acid sites of catalysts. This was operated in transmittance mode on a Bruker Vertex 70 FTIR spectrometer. Pyridine was used as a probe molecule for quantitative analysis of surface acidity of supports and catalysts by FTIR spectroscopy. Powdered samples of catalysts were soaked in a small amount of pyridine and then dried in an oven and the analysis was done in the spectrometer. After exposing the catalyst sample to pyridine vapors and then degassing at 70 °C to remove residual pyridine, the spectroscopic study was done in a Bruker Vertex 70 FTIR spectrometer.

3.2.6 X-ray photoelectron spectroscopy (XPS)

XPS characterization technique was used to determine the chemical state, bonding type, and concentration of various elements present in prepared catalysts. XPS analysis always requires an ultra-high vacuum in the range of $x10^{-9}$ Torr which can be reached in a small chamber. The working of the instrument is displayed in Figure 3.2. The measurements were carried out in Saskatchewan Structural Science Centre (SSSC) using the AXIS Supra (Kratos Analytical, Manchester, UK) XPS instrument. The 500 mm Rowland circle monochromatic Al K-α (1486.6 eV) source. All survey scan spectra were collected in the binding energy range of 0 eV to 1275 eV with a pass energy of 160 eV and 1 eV step. For high-resolution scans, a pass energy of 20 eV, and a step of 0.05 eV were used. Furthermore, multiple scans had been done on the samples to minimize the noise and check the reproducibility, and finally, Casa XPS software version 2.3.18 was used to analyze the obtained spectrum for the required results.
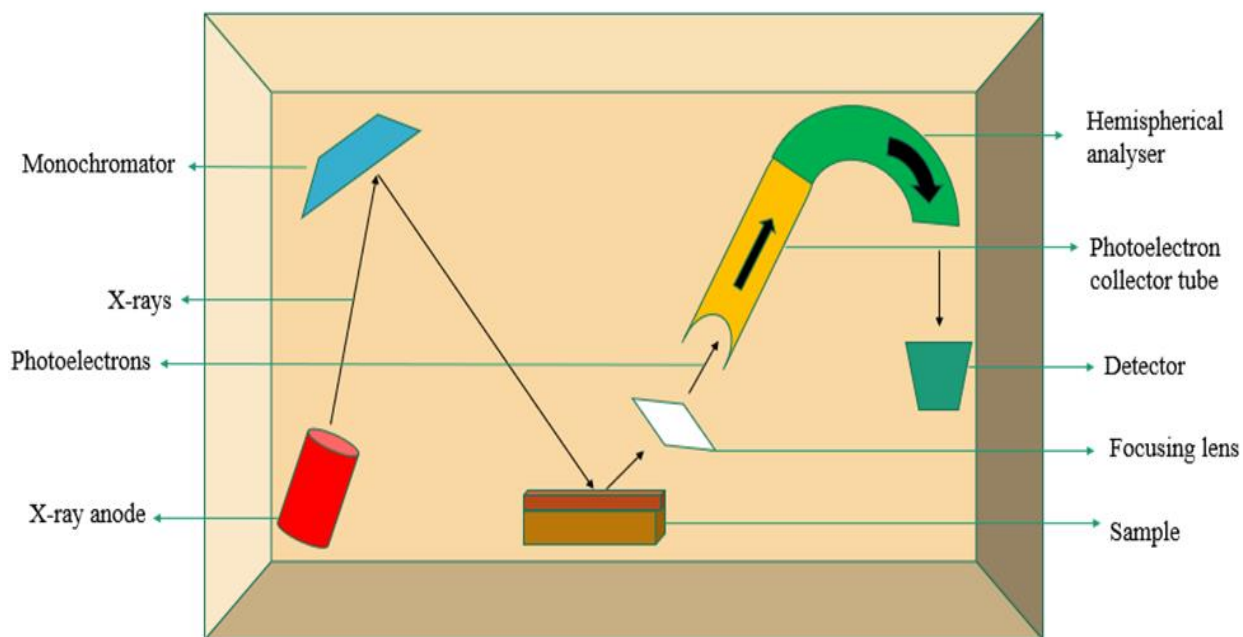
Figure 3. 2 Schematic representation of X-ray photoelectron spectroscopy instrument

3.2.7 Scanning electron microscopy (SEM)

SEM was used to gather morphological information about the prepared catalyst. It is a major non-destructive technique. SEM uses an electron beam to create images of the samples under study. The analysis was done in Western Canada's regional veterinary college at the University of Saskatchewan using the Hitachi SU8010 Field-Emission Scanning electron microscope (Hitachi High-Technologies Corporation, Tokyo, Japan) and the electron gun operated at 12 kV. It provided ultra high-resolution images with high magnification mode ranging from 100x-800,000x which was quite useful in studying the morphology of the sample in detail. The catalyst grains were dispersed onto double carbon tape on the SEM stub. The stub was set into the sample chamber of Quorum Q150T ES coater (Quorum Technologies Inc., Laughton, U.K.). The sample was coated with 5nm Cr with sputtering.

3.3 Catalytic oxidative desulfurization

The catalytic oxidative desulfurization experiments were performed in a 250 mL batch reactor,4843 Parr reactor (Parr Instrument Company, Moline, USA), system equipped with a

heater and temperature and pressure controller. A schematic diagram of the setup is shown in Figure 3.3. In a typical run, 20 g of the feedstock was weighed into the stainless-steel reactor vessel and 1 g catalyst was added. Subsequently, 7 g of H_2O_2 (30% v/v) was added as an oxidant and stirred at 550 rpm at 70°C for 2 h. After the reaction, the vessel could cool to room temperature before filtration to recover the solid catalyst. The bi-phasic (oil and water) reaction products were separated using a separatory funnel due to their density differences.

Subsequently, solvent extraction of the oxidized sulfur compounds (sulfoxides and sulfones) was done using methanol (Fisher Chemical, Saskatoon, Canada) as the extracting solvent as shown in Figure 3.4. In a typical extraction protocol, 10 mL methanol was to the oil-phase in a separatory funnel, vigorously agitated, and allowed to settle for 2 h. The two phases were formed, with oil at the bottom and the solvent and dissolved sulfoxides and sulfones at the top.
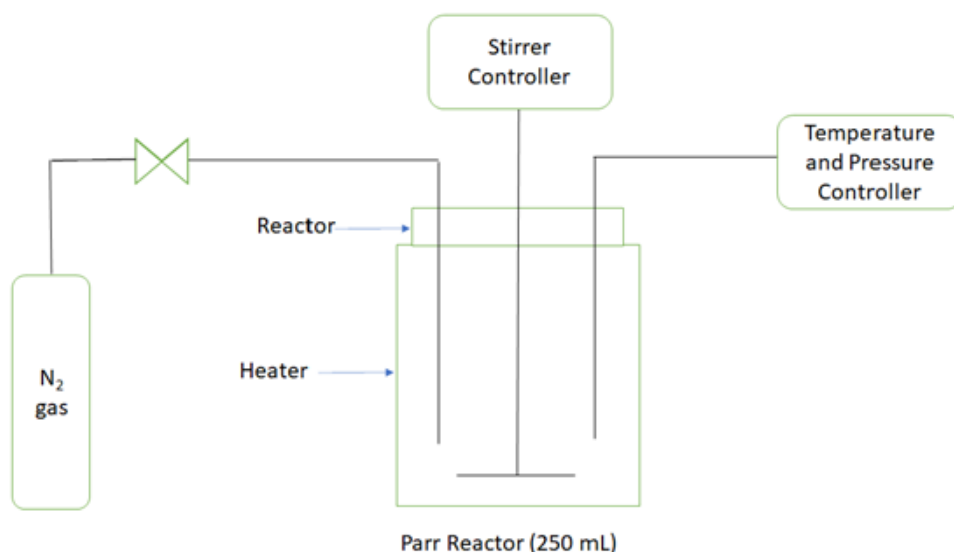

Figure 3. 3 Schematic diagram of Parr reactor set-up for ODS experiments

The separated phases can be seen in Figure 3.4. The oil phase was collected into 20 mL screw-cap vials and kept tightly sealed in the refrigerator for sulfur analysis using the Antek 9000 N/S analyzer.

Figure 3. 4 Solvent extraction process

3.4 Process parameter optimization

The central composite design (CCD) option in Design-Expert Software was used to design experiments considering process parameters such as Temperature, Catalyst/ Oil mass ratio, and Oxidant/Sulfur (O/S) molar ratio. A certain set of experiments were designed to explore the influence of process parameters and their combined effect on the ODS process. Some of the experiments were repeated to check the reproducibility of the results. The main objective was to set a trend among process conditions that would result in a high desulfurization rate. The optimized process conditions obtained for the ODS process were ascertained.

3.5 Oxidative desulfurization kinetic study

Process parameter optimization study does not explore the kinetics of ODS reaction. Kinetic parameters most likely reflect that the key step in the oxidation of sulfur refractory compounds involves both catalyst and sulfur compounds in the feed. The experiment conducted is classified as a three-phase heterogeneous reaction as it includes organic phase fuel, hydrogen peroxide as an oxidant (aqueous phase), and solid-phase catalyst (Sengupta *et al.,* 2012). The kinetic study was investigated with the optimum catalyst at different reaction times. The kinetic parameters were also calculated to show the perfect fit of the model.

3.6 Spent catalyst regeneration

The catalyst deactivation study is very important for industrial feasibility. The spent catalyst filtered out after the ODS reaction was washed with the solvent followed by drying and calcination to remove impurities. The spent catalyst regeneration study was done at least 3 times to observe the change in sulfur removal efficiency (wt%). XRD was performed for the regenerated catalysts to compare them with the fresh catalyst to study the change in spectra and behaviour after every run.

3.7 Summary

The research methodology adopted for the ODS of tire pyrolysis oil using heteropolyacid loaded mesoporous alumina and TUD-1 catalysts includes preparation of supports and catalysts with different Ti/Al and Ti/Si ratios followed by their physicochemical characterization and ultimately using the prepared catalysts in ODS runs. The impact of individual parameters and their collective influence on ODS were studied by the central composite design (CCD) tool. This research provides an insightful study of developed kinetics and also, catalyst regeneration to make it a viable industrial process.

Chapter 4: Oxidative desulfurization runs with HPMo-loaded Ti incorporated mesoporous materials

Most of the content of this chapter has been published as a research article:

Kaur, J., Vedachalam, S., Boahene, P., & Dalai, A. K. (2021). Oxidative Desulfurization of Tire Pyrolysis Oil over Molybdenum Heteropolyacid Loaded Mesoporous Catalysts. Reactions, 2(4), 457–472. http://dx.doi.org/10.3390/reactions2040029.

This chapter includes my contribution towards phase 1 of this research which comprises of synthesis of HPMo-loaded Ti incorporated mesoporous materials and their characterization. Furthermore, subsequent screening tests to optimize the catalyst and oxidant for the ODS of tire pyrolysis oil.

4.1 Synthesis of Ti- Al_2O_3 supports and HPMo supported catalysts

Titania–incorporated mesoporous Al_2O_3 supports were prepared by following the synthesis method mentioned in the literature with few modifications (Lesaint *et al.,* 2008). The chemicals used were Pluronic F127, ethanol (EtOH), isopropanol (iPrOH), aluminum tert-butoxide ($C_{12}H_{27}AlO_3$), titanium isopropoxide ($C_{12}H_{28}O_4Ti$), and water (H_2O). These chemicals were combined as further discussed below following a molar ratio of $1C_{12}H_{27}AlO_3$:$1F127$:$8EtOh$:$6iPrOH$:$2H_2O$ in addition to titanium isopropoxide based on the required Ti/Al molar ratio. Typically, an appropriate amount of Pluronic F127 was added in isopropanol and ethanol solution under continuous stirring at 50 °C which was followed by the addition of aluminum tert-butoxide. The resulting solution was then stirred for about 30 min and then the required amount of titanium isopropoxide was added dropwise and stirred for 30 min. Finally, the calculated quantity of water was added dropwise and stirred for another 15 min. The resultant gel was kept overnight at room temperature. The gel was transferred into an autoclave and heated at 80 °C for 48 h. After hydrothermal treatment, the resulting material was filtered and then calcined in a muffle furnace at 550 °C for 6 h to remove the F127 surfactant. A series of titania-incorporated mesoporous Al_2O_3 supports with Ti/Al of 0, 0.0125, 0.025, and 0.05 was prepared by this one-pot synthesis approach.

Heteropolymolybdic acid (HPMo)-loaded Ti-Al_2O_3 catalysts were prepared by an incipient wet impregnation technique. The prepared supports were loaded with 20 wt% of HPMo using an

aqueous solution of phosphomolybdic acid hydrate. The loaded support was dried for 6 h at 100 °C and calcined at 400 °C for 2 h with a ramp rate of 1°C/min. The final catalysts are labeled as HPMo/Ti-Al$_2$O$_3$(X), where X represents the molar ratio of Ti/Al.

4.2 Synthesis of Ti- TUD-1 supports and HPMo supported catalysts

Titania–incorporated TUD-1 supports preparation was done by the sol-gel method mentioned in the literature with slight changes (Shan *et al.,* 2001). Typically, 20 g of tetraethyl orthosilicate was added to the calculated amount of titanium butoxide and with continuous stirring, for 15 min. 14.3 g of triethanolamine was dissolved in this mixture and vigorously stirred for 1 h, and then 5 g of deionized water was mixed dropwise and stirred for 30 min. Finally, the addition of 13 g of tetraethylammonium hydroxide solution (35 wt % in H$_2$O) was done along with 2 h of stirring. A gel was formed to which ageing was done at 30 °C for 24 h. The resultant mixture was dried at 100 °C for 24 h. After drying, the material was transferred in an autoclave at 200 °C for 6 h for hydrothermal treatment and then calcination was done at 600 °C for 6 h with a ramp rate of 1°C/min. Based on this procedure, four different TUD-1 supports with Ti/Si of 0, 0.0125, 0.025, and 0.05 were prepared.

For the preparation of Ti-TUD-1 catalysts, the prepared supports were loaded with 20 wt% of HPMo using phosphomolybdic acid hydrate. Typically, a required amount of methanol solution of phosphomolybdic acid hydrate was slowly added to TUD-1 support. The mixture was dried at 100 °C for 4 h and then calcination was done in a muffle furnace at 400 °C for 2 h with a ramp rate of 1°C/min. The catalysts prepared based on TUD-1 are denoted as HPMo/Ti-TUD-1(X), where X is Ti/Si molar ratio.

4.3 Oxidative desulfurization process and its mechanism

Preliminary catalyst screening tests were done using hydrotreated light gas oil (HT-LGO) due to the limited availability of tire pyrolytic oil. HT-LGO contains a sulfur content of 0.6 wt.%, which is similar to the sulfur content of tire pyrolysis oil. The catalyst screening experiments were performed under similar ODS conditions: T=70°C, time = 2 h, oxidant/sulfur molar ratio = 10, catalyst loading = 5 wt.%, stirring speed = 550 rpm in a 250 mL Parr batch reactor. The most active catalyst in each series was applied for ODS of tire pyrolysis oil, which contains a sulfur content of

0.72 wt.%. Furthermore, the effectiveness of different oxidants namely hydrogen peroxide, tert-butyl hydroperoxide, and cumene hydroperoxide was evaluated at the above-mentioned process conditions. In a typical catalytic ODS run, after the completion, the reactor was cooled down to room temperature, and all the gases were vented out. The biphasic reaction mixture was filtered to remove the catalyst, and then aqueous and oil phases were separated using a separating funnel. The oxidized sulfur species from the oil phase were removed by solvent extraction using methanol. Methanol was found to be the best solvent as mentioned in the literature for the extraction of oxidized compounds because of its sufficient polarity, volatility, and low cost (Guth *et al.,* 1973). The ODS product sample was analyzed for sulfur using the Antek 9000 N/S analyzer as per the ASTM 5453 method.

Figure 4.1 shows the ODS mechanism for HPMo/Ti-TUD-1 catalyst. This catalyst system consists of $[PMo_{12}O_{40}]^{3-}$ Keggin ions. From the previous research done in our group, it was found that Mo with Keggin type species performed better in terms of desulfurization rate as compared to octahedral MoO_3 species due to more oxygen vacancies in the former than latter (Vedachalam *et al.,* 2020). The Keggin type Mo tends to react with the oxidant i.e H_2O_2 to form hydroperoxymolybdate due to nucleophilic attack. Hydroperoxymolybdate further loses H_2O molecule and forms peroxymolybdate species which is a high-strength electrophile. The sulfur species in the oil attacks the active sites of peroxymolybdate ion by the nucleophilic attack and releases one of its oxygen and ends up being oxidized. Sulfoxides can be either further oxidized to sulfones in the presence of peroxomolybdenum or desorbed from the catalyst site (Ghubayra *et al.,* 2019). In this case, we have excess oxidant in the system the cycle continues. Furthermore, Ti incorporation in the catalyst also forms Lewis acid sites which boost the ODS reaction of HPMo by further withdrawing the electrons from peroxymolybdate species and making it even more strong electrophile to attack organosulfur compounds. The sulfoxides and sulfones formed by reacting with oxidant, are polar in nature which can be easily extracted by polar solvents (Vedachalam *et al.,* 2020).
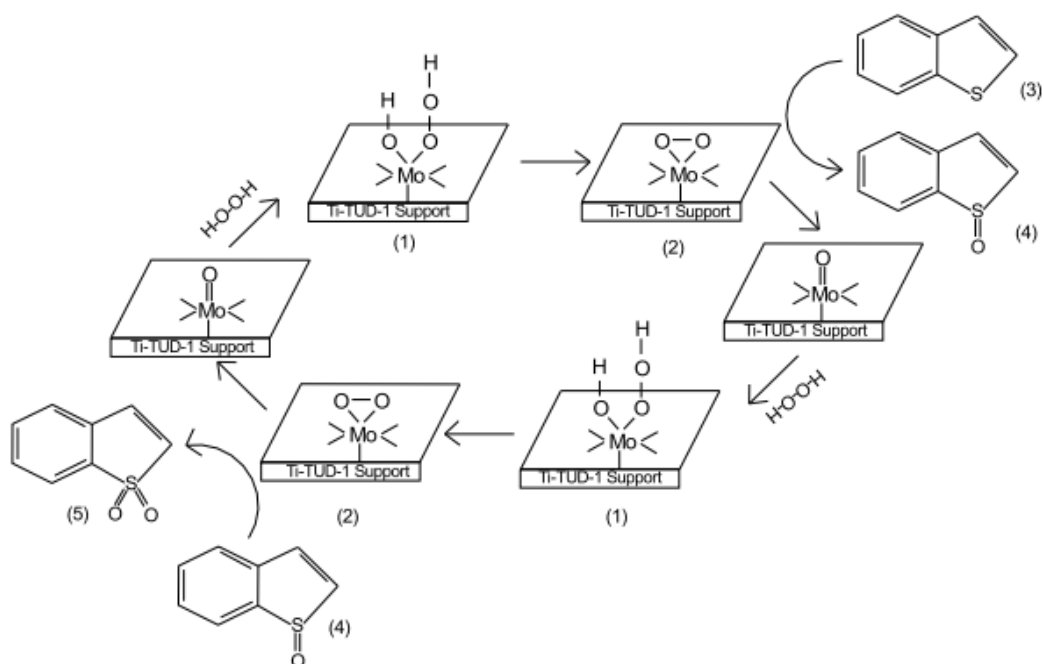
Figure 4. 1 ODS mechanism with Keggin type Molybdenum loaded HPMo/Ti-TUD-1 catalyst (Vedachalam *et al.,* 2020)

4.4 Results and discussion

4.4.1 Catalyst characterization

X-ray diffraction analysis

XRD analysis was performed in the wide-angle range (2θ = 10 to 90°) with a Bruker AXS D8 diffractometer. Please refer to Section 3.2.1 for a detailed procedure.

The wide-angle XRD spectra depicted in Figure 4.2 show the fingerprint of Keggin-type phosphomolybdic acid in the HPMo/Ti-TUD-1 type catalysts (L. Marosi *et al.,* 2000). These Keggin ion peaks are absent in HPMo/Ti-Al$_2$O$_3$ catalysts. Alumina peaks are observed in Ti- Al$_2$O$_3$ supports as well as catalysts at 37, 46, and 67°. Ti-TUD-1 (0,0.5,0.025,0.0125) supports show a broad amorphous silica peak at 15-30° range (Telalović *et al.,* 2010)(Shan *et al.,* 2001). The basic OH groups of Al$_2$O$_3$ are known to interact with phosphomolybdic acid and thus lead to depolymerization of polyoxometallate anion (Van Veen *et al.,* 1990). Due to depolymerization, the Keggin structure of phosphomolybdic acid is not preserved on Ti-Al$_2$O$_3$ support, unlike Ti-TUD-1. The absence of characteristics peaks of titania at 2 theta angles of 25.4° and 48° (sharp

intense peaks) and minor peaks at 36.9,37.7, 38.5, 53.8, 55.0, 62.0, and 62.6° in both types of supports evidence non-existence of extra framework titania. The XRD pattern of HPMo/Ti-TUD-1 catalysts is very similar to the pure phosphomolybdic acid XRD pattern. Thus, it can be concluded that the keggin structure of HPMo acid has been preserved on Ti-TUD-1 supports (L. Marosi *et al.,* 2000)(Vedachalam *et al.,* 2020).
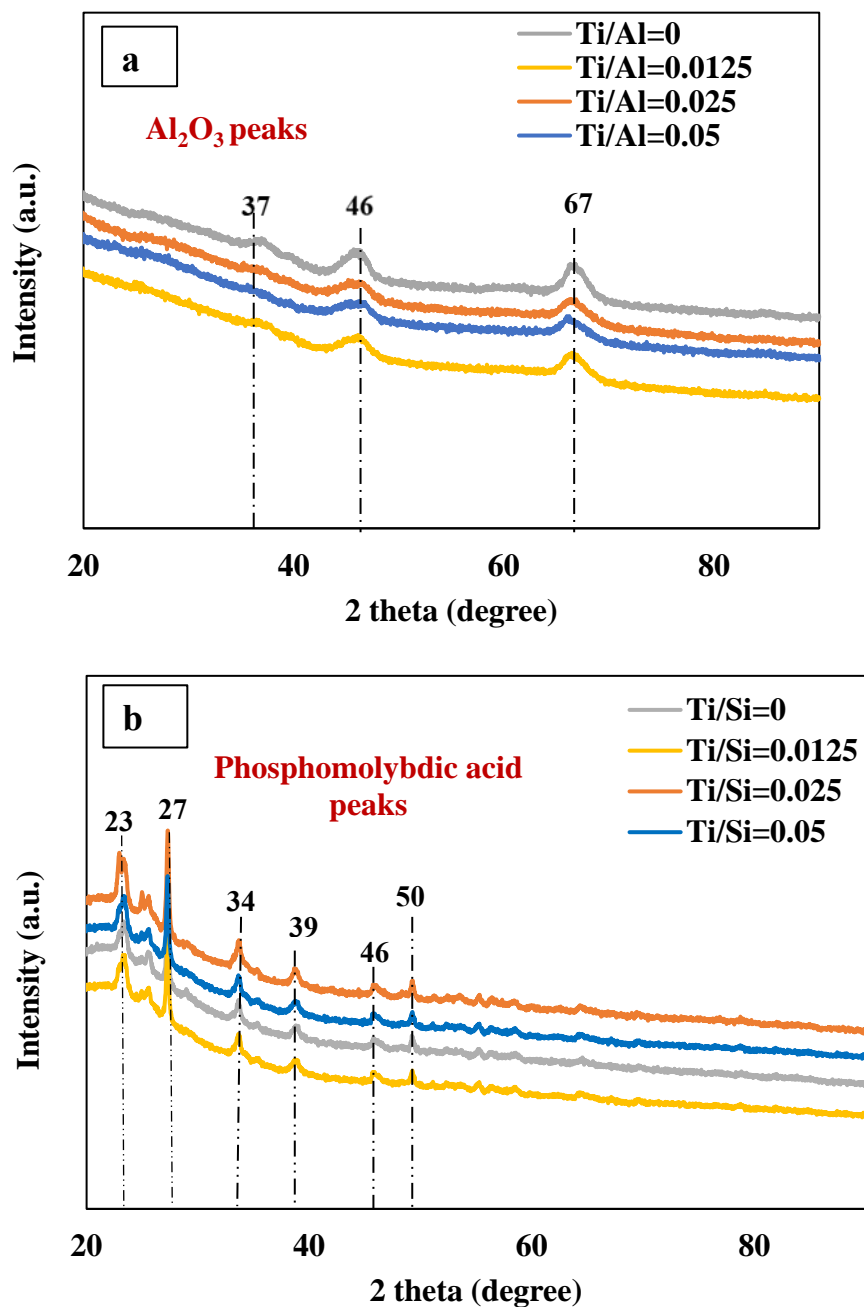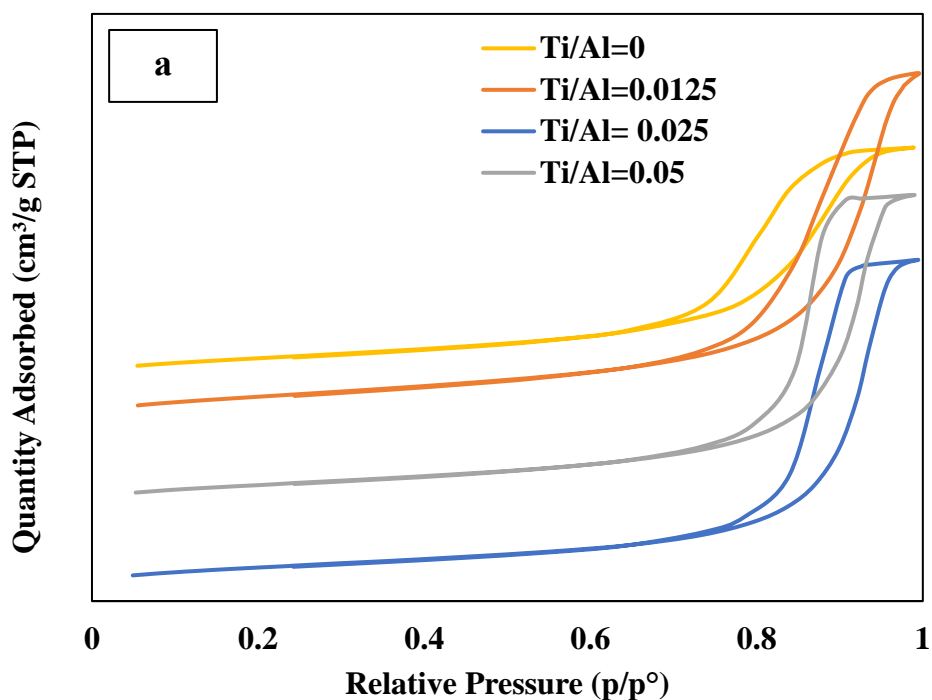

Figure 4. 2 XRD spectra of (a) HPMo/Ti-Al$_2$O$_3$ and (b) HPMo/Ti-TUD-1 catalysts

Nitrogen adsorption-desorption isotherms

The textural properties such as surface area, pore-volume, and pore diameter of the Ti-Al$_2$O$_3$ and Ti-TUD-1 supports and their corresponding HPMo supported catalysts were measured using a Micromeritics ASAP 2020 instrument. Please refer to Section 3.2.2 for a detailed procedure. Nitrogen adsorption-desorption isotherms of HPMo/Ti-Al$_2$O$_3$ and HPMo/ Ti-TUD-1 catalysts are shown in Figure 4.3. Both types of catalysts show the Type IV isotherm with an H1 hysteresis loop that is characteristics of mesoporous materials. Textural properties such as BET surface area, pore-volume, and BJH pore diameter of supports and their respective catalysts as determined by nitrogen physisorption are given in Table 4.1. The phosphomolybdic acid loading reduces the surface area and pore volume of supports significantly due to the filling of mesopores by Keggin anion (large cluster of twelve MO$_6$ octahedra), which has a kinetic diameter of around 1.2 nm (Vedachalam *et al.,* 2020).
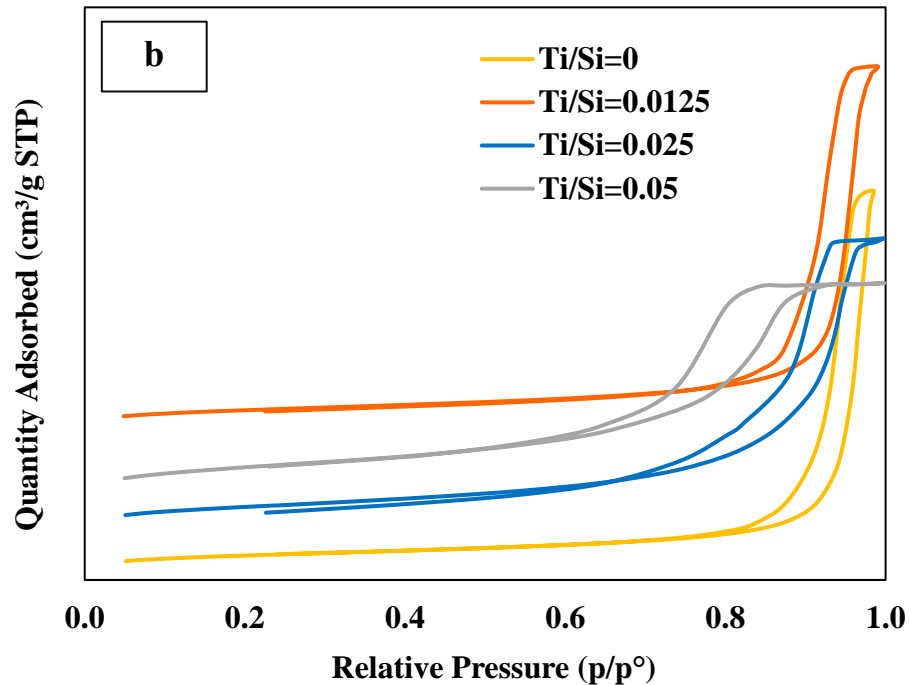
Figure 4. 3 N_2 isotherm of (a) HPMo/Ti-Al$_2$O$_3$ and (b) HPMo/Ti-TUD-1 catalysts

Table 4. 1 Textural properties of supports and catalysts

Sample ID	BET surface area (m²/g)	Pore volume (cm³/g)	BJH pore diameter (nm)
Ti-Al$_2$O$_3$ (Ti/Al= 0)	361	1.4	10.1
Ti-Al$_2$O$_3$ (Ti/Al = 0.0125)	387	1.9	14.0
Ti-Al$_2$O$_3$ (Ti/Al = 0.025)	374	1.8	14.4
Ti-Al$_2$O$_3$ (Ti/Al = 0.05)	388	1.7	12.9
HPMo/Ti-Al$_2$O$_3$ (Ti/Al = 0)	279	0.9	9.4
HPMo/Ti-Al$_2$O$_3$ (Ti/Al = 0.0125)	310	1.3	13.4
HPMo/Ti-Al$_2$O$_3$ (Ti/Al = 0.025)	280	1.3	14.1
HPMo/Ti-Al$_2$O$_3$ (Ti/Al = 0.05)	271	1.2	12.2

Ti-TUD-1 (Ti/Si = 0)	356	1.8	25.1
Ti-TUD-1 (Ti/Si = 0.0125)	352	1.9	21.7
Ti-TUD-1 (Ti/Si = 0.025)	432	1.5	14.0
Ti-TUD-1 (Ti/Si = 0.05)	608	1.3	7.8
HPMo/Ti-TUD-1 (Ti/Si = 0)	234	1.5	26.9
HPMo/Ti-TUD-1 (Ti/Si = 0.0125)	254	1.7	22.1
HPMo/Ti-TUD-1 (Ti/Si = 0.025)	311	1.2	13.0
HPMo/Ti-TUD-1 (Ti/Si = 0.05)	406	0.9	7.4

NH$_3$-Temperature programmed desorption

NH$_3$ temperature-programmed desorption (NH$_3$-TPD) analysis was done in a ChemBET-3000TPR/TPD analyzer. Please refer to Section 3.2.3 for a detailed procedure.

The strength of acidic sites corresponds to their desorption temperature. The acidic sites are categorized as shown in Table 4.2.

Table 4. 2 Acidic strength for the corresponding temperature in NH$_3$-TPD

| No.	Acidic strength	Temperature (°C)
1	Weakly acidic	$< 200\ °C$
2	Acidic	200 °C to 350 °C
3	Strongly acidic	$> 350\ °C$

The NH$_3$ desorption profiles of both series of catalysts comprised a major peak between 120 to 300 °C and a small peak between 300 to 450°C (Figure is not shown). These peaks correspond to weak and medium acid sites, respectively. The total acid sites on the catalysts were quantified and given in Table 4.3. The amount of acid sites is gradually increasing with an increase in the Ti content of catalysts.

Table 4. 3 NH$_3$-TPD data for Ti-Al$_2$O$_3$ and Ti-TUD-1 supports and catalysts

Sample ID	Peak Number	Maximum temperature (°C)	Quantity of Active Acid sites (mmol/g)	Total Active acid sites (mmol/g)
Ti-Al$_2$O$_3$	1	175	0.19	
(Ti/Al = 0)	2	378	0.32	0.51
Ti-Al$_2$O$_3$	1	92	0.26	
(Ti/Al = 0.0125)	2	528	0.22	0.48
Ti-Al$_2$O$_3$	1	180	0.22	
(Ti/Al = 0.025)	2	373	0.30	0.52
Ti-Al$_2$O$_3$	1	163	0.17	
(Ti/Al = 0.05)	2	374	0.16	0.33
HPMo/Ti-Al$_2$O$_3$	1	250	0.21	
(Ti/Al = 0)	2	81	0.11	0.32
HPMo/Ti-Al$_2$O$_3$	1	283	1.04	
(Ti/Al = 0.0125)	2	470	0.27	1.31
HPMo/Ti-Al$_2$O$_3$	1	285	0.81	
(Ti/Al = 0.025)	2	511	0.21	1.02
HPMo/Ti-Al$_2$O$_3$	1	165	0.22	
(Ti/Al = 0.05)	2	356	0.19	0.41
Ti-TUD-1 (Ti/Si = 0)	1	162	0.04	0.04
Ti-TUD-1	1	88	0.16	
(Ti/Si = 0.0125)	2	120	0.13	0.29
Ti-TUD-1 (Ti/Si = 0.025)	1	393	0.05	0.05
Ti-TUD-1	1	99	0.43	
(Ti/Si = 0.05)	2	149	0.26	0.69
HPMo/Ti-TUD-1 (Ti/Si = 0)	1	167	0.21	0.21
HPMo/Ti-TUD-1	1	108	0.40	
(Ti/Si = 0.0125)	2	206	0.33	0.73
HPMo/Ti-TUD-1	1	156	0.12	
(Ti/Si = 0.025)	2	597	0.02	0.14
HPMo/Ti-TUD-1	1	127	0.79	
(Ti/Si = 0.05)	2	234	0.50	1.29

Fourier Transform Infrared Spectroscopy (FTIR)

FTIR analysis was done to confirm the presence of functional groups present in the prepared supports and catalysts. Bruker Vertex 70 FTIR spectrometer (Bruker Optics Inc, Billerica, USA) instrument was used for operating the analysis as mentioned in Section 3.2.4. FTIR spectra for mesoporous Mo-loaded catalysts are shown in Figure 4.4. In Figure 4.4 a, broadband from 490 to 1000 cm^{-1} can be observed in all Al_2O_3 catalysts. It could correspond to Al-O vibration (Badoga *et al.,* 2014). However, in Figure 4.4 b bands with wavenumber 1200 and 1080 cm^{-1} are because of asymmetric stretching of SiO_4 tetrahedral units in silicate structures, while the band at 805 cm^{-1} are due to the symmetric vibration of the same units (Shan *et al.,* 2001). The main objective of this analysis is to find the Al-Ti and Si-Ti bonds to ensure Ti incorporation in the framework. The presence of Ti ions can be confirmed by observing the band at 955 cm^{-1} in Figure 4.4 b because of Ti-O-Si vibration (Shan *et al.,* 2001). The low intensity of Ti peaks in Figure 4.4 can be explained due to the low amount of incorporated Ti.
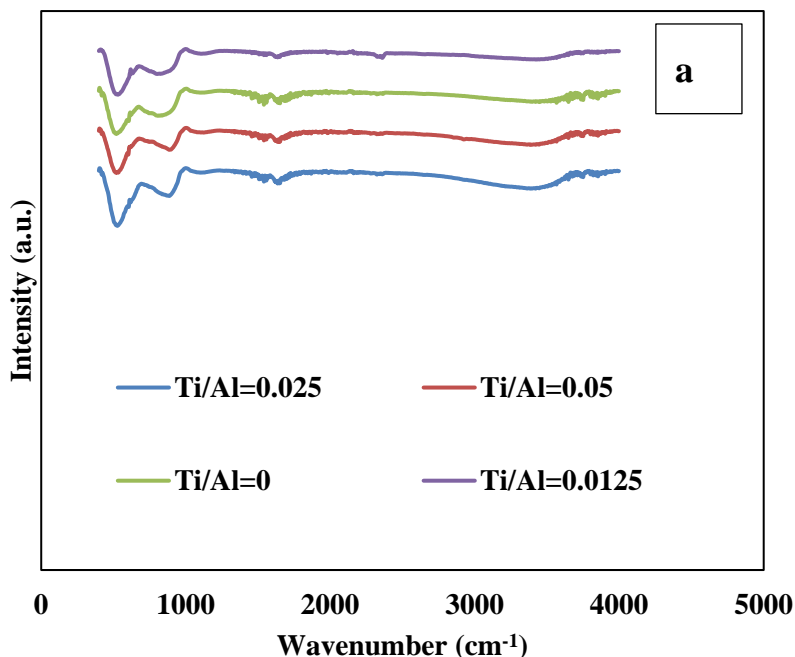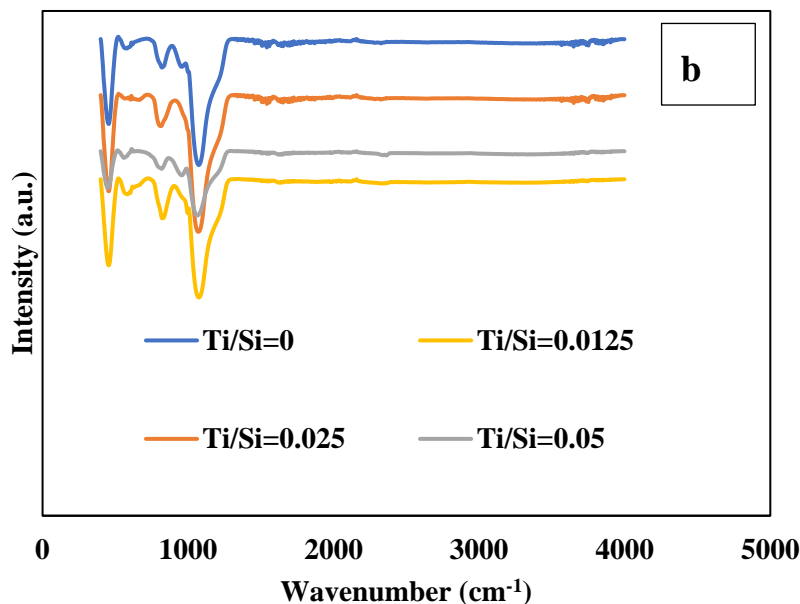
Figure 4. 4 FTIR spectra of a) HPMo/Ti- Al_2O_3 catalysts and b) HPMo/Ti-TUD-1 catalysts

Pyridine Fourier Transform Infrared Spectroscopy (Pyridine FTIR)

Fourier transform infrared spectroscopy with pyridine (Pyridine FTIR) as a probe molecule was used for differentiating Lewis and Brønsted acid sites of catalysts. The catalyst sample was exposed to pyridine vapors and then degassed at 70 °C to remove residual pyridine and then the spectroscopic study was done in a Bruker Vertex 70 FTIR spectrometer. Please refer to Section 3.2.5 for a detailed procedure.

A Lewis acid is any material that can accept an electron pair. However, Brønsted acid tends to donate a proton (Cui *et al.,* 2020). Pyridine FTIR analysis determined the Lewis and Brønsted acidic sites of catalysts and the spectra are shown in Figure 4.5. Pyridine adsorption on HPMo/Ti-Al_2O_3 and HPMo/Ti-TUD-1 series results in bands at 1448, 1539, 1488 cm^{-1}, which are characteristic of Lewis acid, Brønsted acid, and overlap of Brønsted and Lewis acid sites, respectively (Badoga *et al.,* 2014). The pyridine FTIR study confirms that HPMo/Ti-Al_2O_3 and HPMo/Ti-TUD-1 catalysts contain both Brønsted and Lewis acid sites.
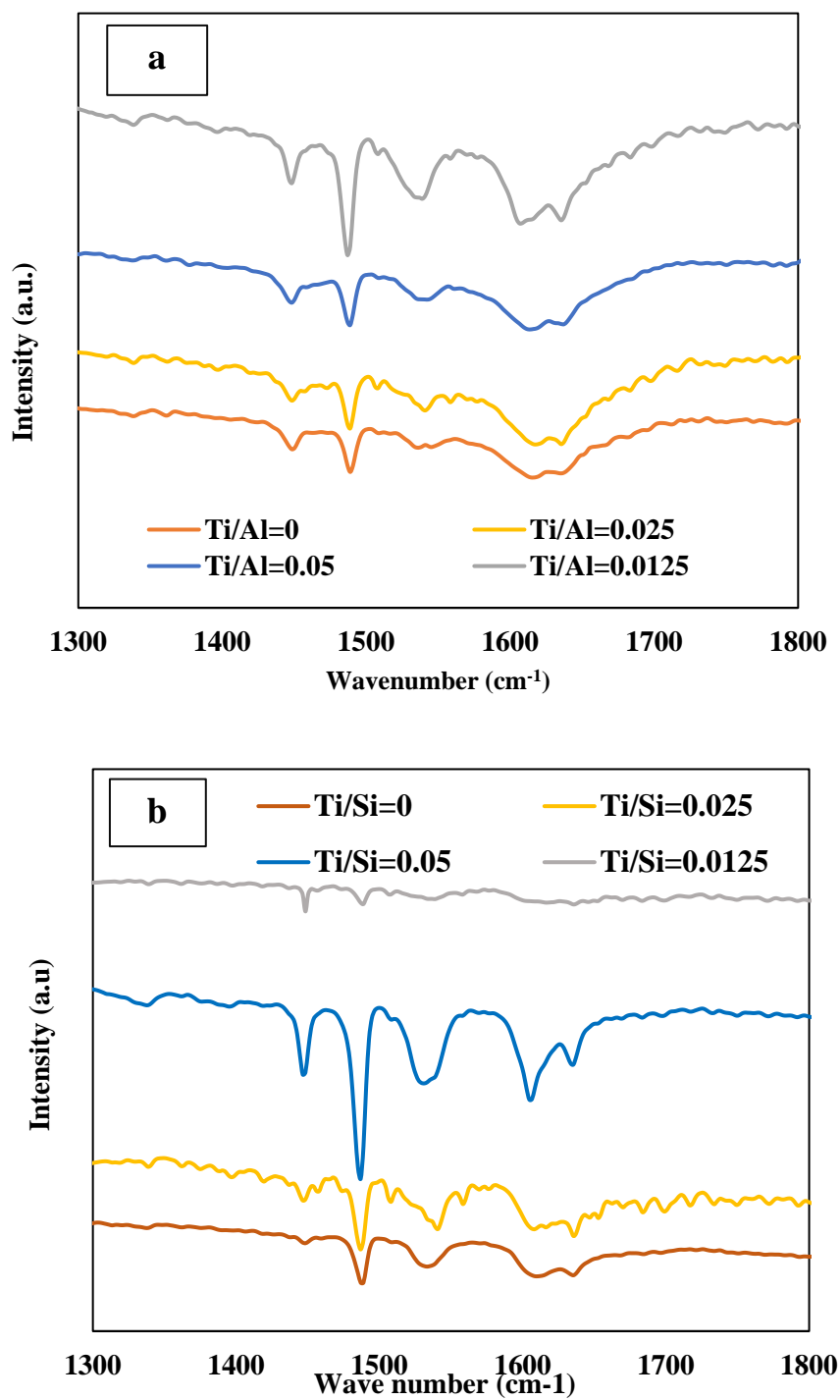
Figure 4. 5 Pyridine-FTIR spectra of (a) HPMo/Ti-Al$_2$O$_3$ and (b) HPMo/Ti-TUD-1 catalysts

X-ray photoelectron spectroscopy (XPS)

The X-ray photoelectron spectroscopy (XPS) data were obtained using a Kratos (Manchester, UK) AXIS Supra system equipped with a 500 mm Rowland circle monochromated Al K-α (1486.6 eV) source. The high-resolution scans of several regions were obtained using 0.05 eV steps and a pass energy of 20 eV. The data was processed with Casa XPS software. Please refer to Section 3.2.6 for a detailed procedure.

X-ray photoelectron spectroscopy was performed to study the chemical states of Ti in HPMo/Ti-Al_2O_3 and HPMo/Ti-TUD-1 catalysts. The Ti 2p core-level spectra of HPMo/Ti-TUD-1 and HPMo/Ti-Al_2O_3 catalysts are shown in Figure 4.6. Generally, the framework and non-framework Ti species exist in the tetrahedral and octahedral coordination, respectively. The binding energies at 458.4 and 464 eV are associated with $2p_{3/2}$ and $2p_{1/2}$ orbital spin electrons of tetrahedral coordinated Ti (IV) species (Vedachalam *et al.,* 2020). The intensities of these peaks are increasing with the Ti loading and appear predominant for the Ti/Si (Al) ratio of 0.05. The XPS result confirms the successful substitution of Ti in the Al_2O_3 and TUD-1 frameworks.
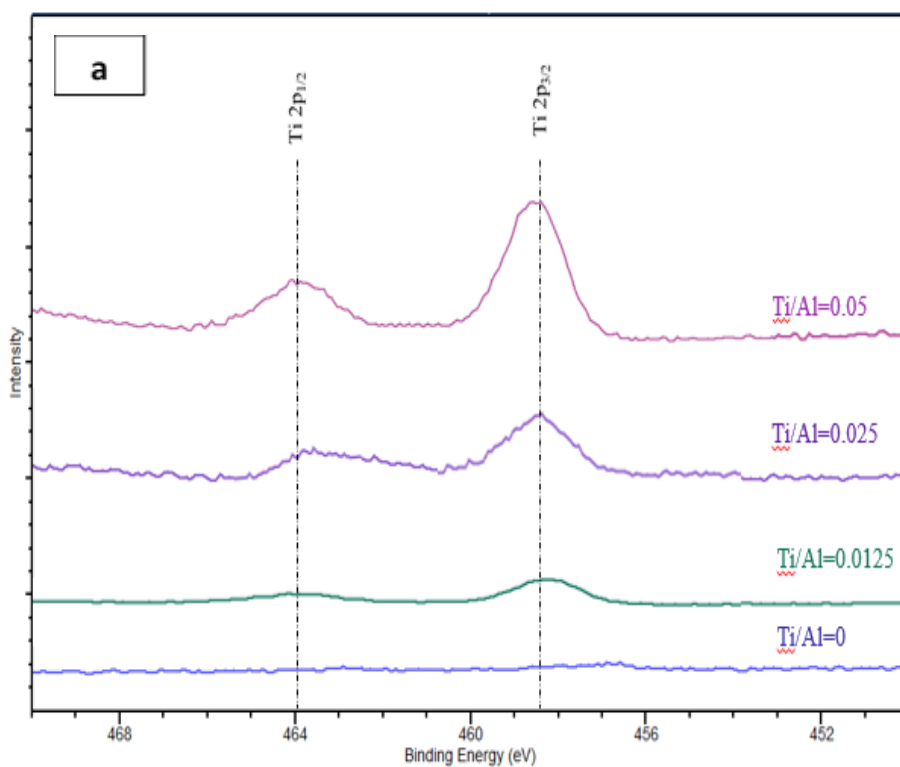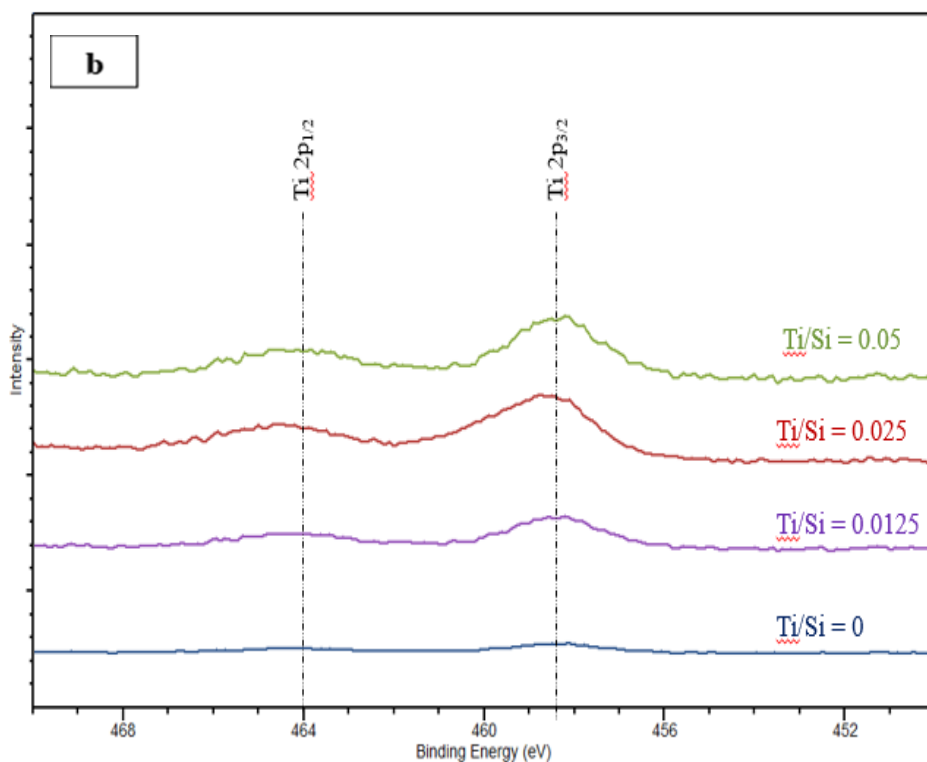
Figure 4. 6 Ti 2p XPS of (a) HPMo/Ti-Al$_2$O$_3$ and (b) HPMo/Ti-TUD-1 catalysts

Scanning electron microscopy (SEM)

The surface morphology of the prepared catalyst was analyzed with the Hitachi SU8010 Field-Emission Scanning electron microscope (FE-SEM). Please refer to Section 3.2.7 for a detailed procedure.

The SEM image of HPMo loaded on Ti-TUD-1 support is presented in Figure 4.7(a). The image shows that the particles have well-defined morphology and the crystals of HPMo loaded over Ti-TUD-1 support are clearly visible. The particle sizes range mainly are in micrometers as studied by (Xia et al. 2017). In this case, the samples consist of about 1-4 µm crystal shaped particles (see Figure A.5). SEM images are in line with the images of Au/Ti-TUD-1 sample presented by (Sinha et al. 2005). In some cases, HPMo impregnated on the support surface leads to particle accumulation (see Figure 4.8(b)).
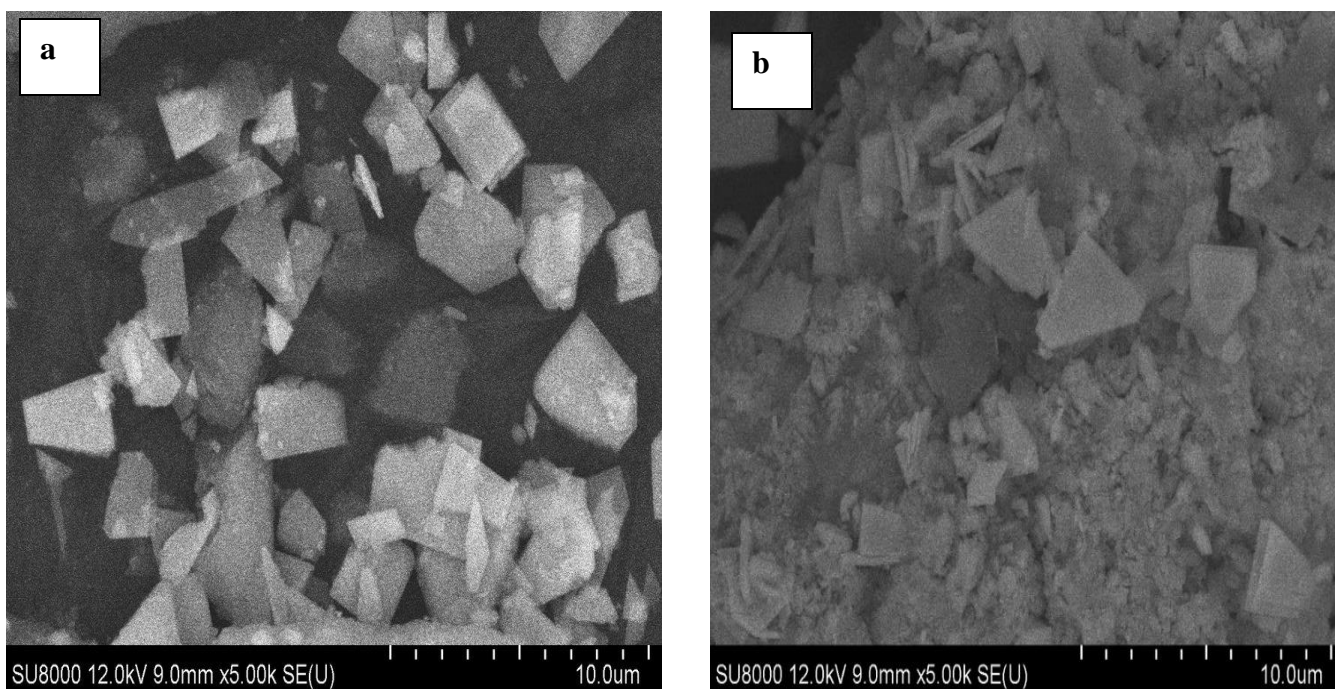
Figure 4. 7 SEM images of HPMo/Ti-TUD-1(Ti/Si=0.025) catalyst

4.4.2 Oxidative desulfurization

Desulfurization of hydrotreated light gas oil over the mesoporous Ti-Al_2O_3 series HPMo catalysts shows maximum sulfur and nitrogen removal with HPMo/Ti-Al_2O_3(0.025) i.e., 54.6% and 76.8%. Similarly, HPMo/Ti-TUD-1(0.025) was found to be the most active catalyst in the TUD-1 series catalyst with 60.4% sulfur removal and 84.8% of nitrogen removal efficiency. The trend shown in Figure 4.8 confirms that the Lewis acidity associated with Ti influences the removal of sulfur by promoting the oxidation activity of HPMo. A similar promotional effect of Ti on the ODS activity of HPMo with heavy gas oil was observed in our earlier study (Vedachalam *et al.,* 2020).

The optimum catalysts of both series, which were identified in ODS of HT-LGO were tested for ODS of TPO. As shown in Figure 4. 9, HPMo/Ti-TUD-1(0.025) shows better ODS activity than HPMo/Ti- Al_2O_3 (0.025) with the highest sulfur removal efficiency of 45.2 ± 3.2 wt.% and nitrogen removal of 79.1 ± 2.6 wt.% respectively
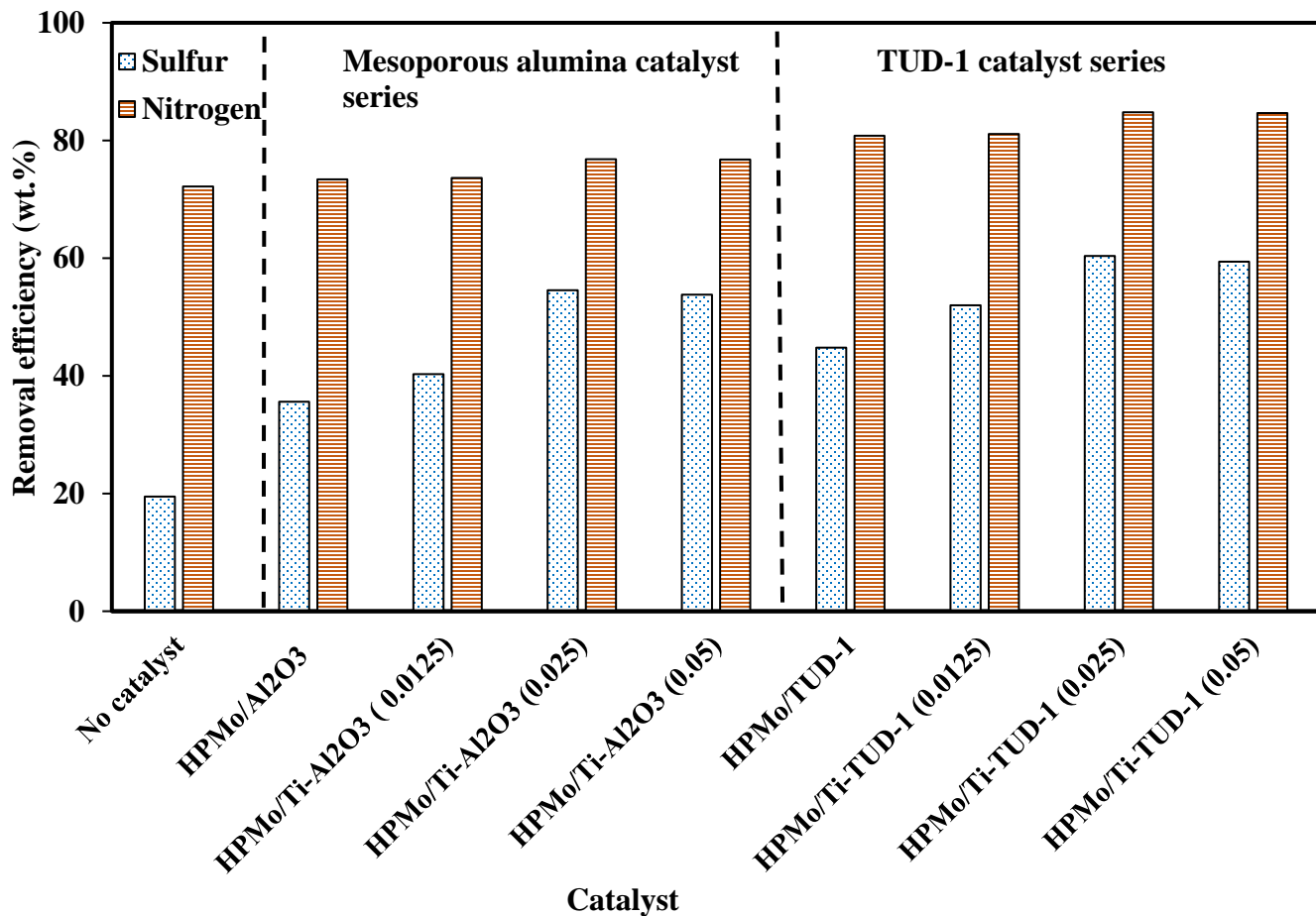
Figure 4. 8 ODS of hydrotreated light gas oil over HPMo/Ti-Al$_2$O$_3$ and HPMo/Ti-TUD-1 catalysts: catalyst/feed ratio of 0.05; Temperature of 70 °C; 30% H$_2$O$_2$ as oxidant; H$_2$O$_2$/Sulfur ratio of 10; reaction time of 2 h; and stirring speed of 550 rpm**.**

The experiments were repeated five times to calculate experimental error through standard deviation. ODS run with Ti-TUD-1 support without HPMo loading was also conducted to observe the effect of heteropolyacid. It was found that the sulfur removal efficiency has increased by 18.4 wt.% with HPMo loading on Ti-TUD-1(0.025) catalyst.
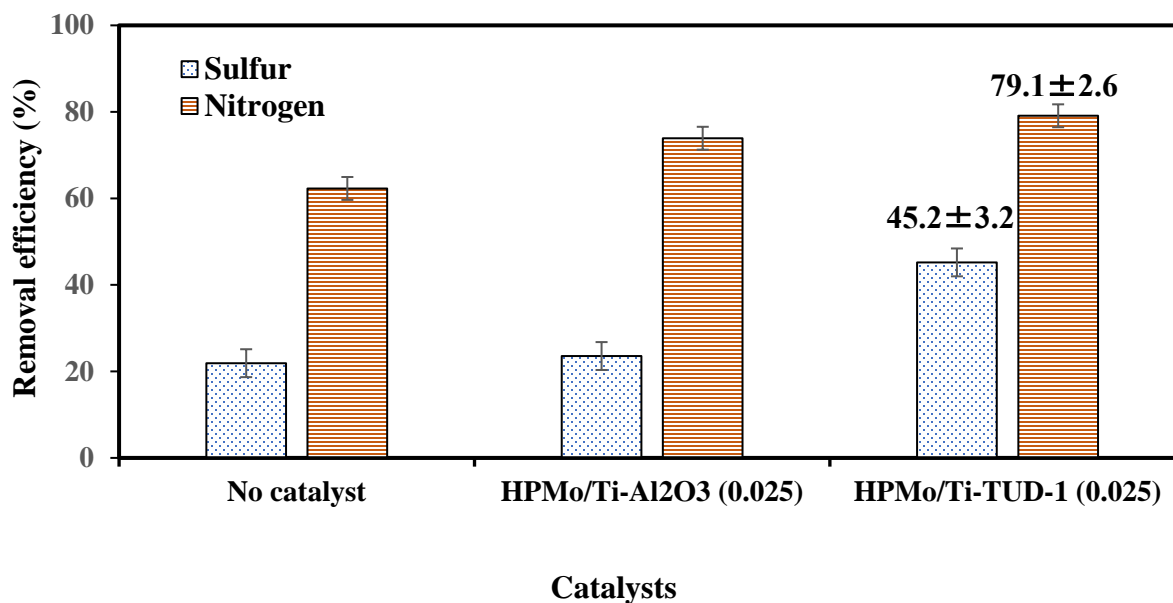
Figure 4. 9 ODS of tire pyrolysis oil over HPMo/Ti-Al$_2$O$_3$ (Ti/Al=0.025) and HPMo/Ti-TUD-1(Ti/Si= 0.025) catalysts: catalyst/feed ratio of 0.05; Temperature of 70 °C; 30% H$_2$O$_2$ as oxidant; H$_2$O$_2$/Sulfur ratio of 10; reaction time of 2 h; and stirring speed of 550 rpm.

Among the prepared catalysts, HPMo/Ti-TUD-1(0.025), which had maximum desulfurization activity with TPO, was used to investigate the efficiency of various oxidants at an O/S molar ratio of 10. During the ODS process, the oxidant provides oxygen to sulfur to form sulfoxide or sulfone. Screening of oxidants such as hydrogen peroxide, tert-butyl hydroperoxide (TBHP), and cumene hydroperoxide was done for ODS of TPO. A blank experiment was also conducted without an oxidant. As shown in Figure 4.10, hydrogen peroxide and cumene peroxide were found to be better oxidants than tert-butyl hydroperoxide for ODS of TPO. However, in the case of oxidation with cumene hydroperoxide, thermal decomposition and fuel instability of hydroperoxide makes sulfones and sulfoxides extraction difficult from the oil phase (Mushrush *et al.,* 1994). Also, as hydrogen peroxide is less expensive than cumene peroxide, further studies were carried using hydrogen peroxide.
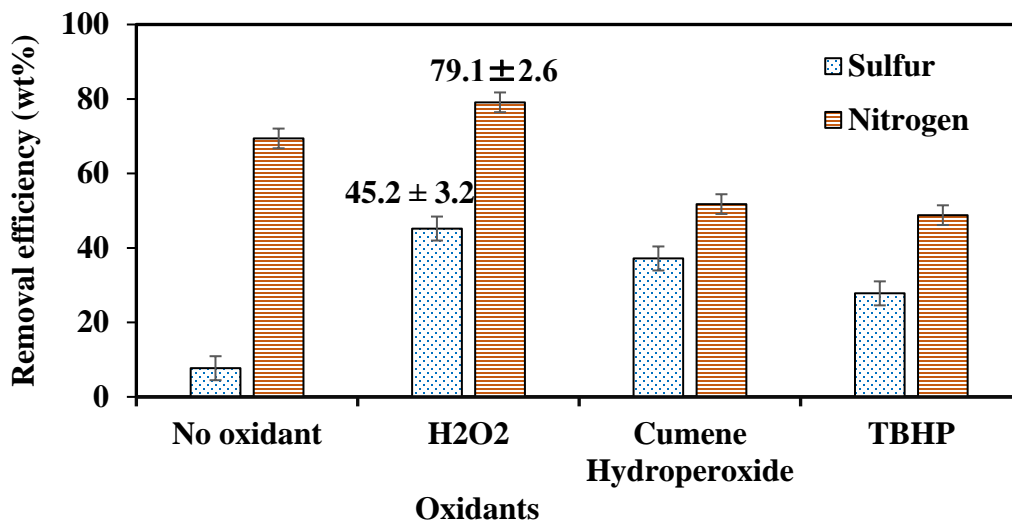
Figure 4. 10 Effects of oxidants on ODS of TPO over HPMo/TiTUD-1 (Ti/Si=0.025) catalyst: catalyst/feed ratio of 0.05; Temperature of 70 °C; oxidant/sulfur (O/S) ratio of 10; reaction time of 2 h; and stirring speed of 550 rpm

4.4.3 ODS of tire pyrolysis oil- Mass balance

In a typical ODS run 20 g of TPO was weighed along with the 7 g of oxidant i.e., H_2O_2 (30% v/v), and 1 g of catalyst (Catalyst/ oil =5wt%) was used. Please refer to Section 3.3 for a detailed procedure. ODS run took place in a CSTR which gives out the oxidized TPO as a product. The oxidized TPO was filtered out to recover the used catalyst. The oxidized TPO was allowed to settle and the unconverted H_2O_2 and H_2O were separated and removed. 18.65 g of oxidized TPO was recovered after decantation as some of the oil (1.35 g) was lost with the spent catalyst. 6.75 wt% of oil was lost until this step. After solvent extraction with methanol the final desulfurized TPO product was weighed 15.46 g. So, by performing the mass balance of ODS of TPO, 77.3 wt% of oil was recovered in total and the rest 22.7 wt% of the oil was separated in the solvent phase along with the mixture of sulfones, sulfoxides, and polar compounds. The mass balance of ODS of TPO has been explained in detail in Figure 4.11.
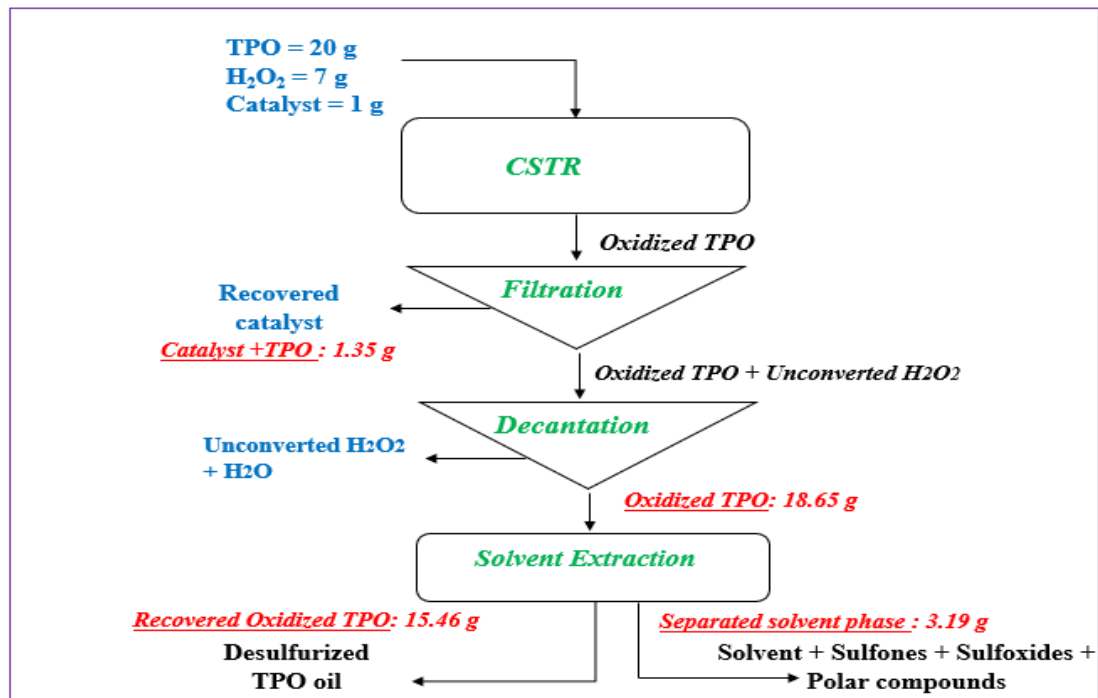
Figure 4. 11 Mass balance of ODS of tire pyrolysis oil

4.5 Conclusions

This phase of the research described the synthesis of Phosphomolybdic acid-loaded titania-incorporated mesoporous Al_2O_3 and TUD-1 catalysts with different Ti/Al and Ti/Si ratios. Mesoporisity of the catalysts was proved by type IV isotherm with H1 hysteresis loop in nitrogen-adsorption-desorption isotherm. XRD analysis proved the preservation of the Keggin structure of phosphomolybdic acid (HPMo) on Ti- TUD-1 supports, unlike Ti-Al_2O_3 supports. Furthermore, pyridine FTIR analysis confirmed the presence of both Brønsted and Lewis acid sites in prepared catalysts. Substitution of Ti inside Al_2O_3 and TUD-1 frameworks was confirmed by XPS spectra. NH_3-TPD analysis proved the rise in acidity on the incorporation of Ti. HPMo/Ti- Al_2O_3 (0.025) and HPMo/Ti-TUD-1(0.025) catalysts have shown the highest sulfur and nitrogen removal efficiencies with HT-LGO. Among the two series of catalysts, HPMo/Ti-TUD-1(0.025) was found to be the most active catalyst for ODS of tire pyrolysis oil with sulfur and nitrogen removal efficiencies of 45.2 ± 3.2 wt.% and 79.1 ± 2.6 wt.%. In the case of TPO, hydrogen peroxide resulted to be the oxidant with the highest removal efficiency rate. As calculated from the mass balance study of ODS of TPO, 3.19 g of oil was separated along with the solvent phase during the solvent extraction.

Chapter 5: Process optimization, kinetic study, and catalyst regeneration

Most of the content of this chapter has been published as a research article.

Kaur, J., Vedachalam, S., Boahene, P., & Dalai, A. K. (2021). Oxidative Desulfurization of Tire Pyrolysis Oil over Molybdenum Heteropolyacid Loaded Mesoporous Catalysts. Reactions, 2(4), 457–472. http://dx.doi.org/10.3390/reactions2040029.

This chapter includes my contribution towards phase 2 of this research which comprises of process parameters optimization study for oxidative desulfurization reaction with the optimized catalyst concluded from Chapter 4, using tire pyrolysis oil. The kinetic study was also included to understand the reaction pathway for oxidative desulfurization reaction. Furthermore, catalyst regeneration and reusability analysis were also performed using the optimized catalyst to help ascertain the durability of the prepared catalyst for the oxidative desulfurization of tire pyrolysis oil application.

5.1 Oxidative desulfurization parameters optimization

The impacts of process conditions on ODS of tire pyrolysis oil were examined over an optimal catalyst concluded from Chapter 4. The process conditions were optimized using the central composite design (CCD) option in Design Expert® software (version 6.0.11, State-Ease Inc., Minneapolis, MN, USA). The ranges of process parameters are displayed in Table 5.1. A set of 20 experiments was designed with a centre point experiment repeated six times as shown in Table 5.2. The repetition was done to check the reproducibility of the experiments under the same parameters (Rana *et al.,* 2017). The feed amount and reaction time was kept constant at 40 g and 2 h, respectively.

Table 5. 1 Optimization parameters and their corresponding range for the central composite design

No.	Process parameters	Range
1	Temp (°C)	35-70
2	Amount of catalyst in oil (wt%)	5-13
3	O/S (molar ratio)	3-10

Table 5. 2 Design of experiment for process optimization

Run	O/S (molar ratio)	Run temperature (°C)	Amount of catalyst in oil (wt%)
1	3.0	35.0	13.0
2	6.5	52.5	9.0
3	6.5	52.5	15.7
4	3.0	35.0	5.0
5	10.0	35.0	13.0
6	6.5	81.9	9.0
7	10.0	70.0	13.0
8	0.6	52.5	9.0
9	6.5	52.5	2.3
10	6.5	52.5	9.0
11	12.4	52.5	9.0
12	6.5	23.1	9.0
13	6.5	52.5	9.0
14	6.5	52.5	9.0
15	6.5	52.5	9.0
16	10.0	35.0	5.0
17	10.0	70.0	5.0
18	3.0	70.0	5.0
19	3.0	70.0	13.0
20	6.5	52.5	9.0

5.2 Analysis of variance (ANOVA)

Analysis of variance (ANOVA) was performed to determine the impact of process parameters to enhance the desulfurization rate in the ODS run. It includes several tests for model verification. F-test (Fisher test) stated how efficient is the chosen model and the impact of process conditions in the final response plots. p-value test statistically checked the significance of process parameters and their influence on each other in the resulting response at a 95% confidence interval. The impact of individual parameters on desulfurization rate was also determined by the sequential sum of squares (SS). Upon dividing the degree of freedom by the sum of squares, the mean square was calculated.

High values of the F-test and sum of squares implement the process parameter's significance relatively. Furthermore, a p-value of more than 5% indicates that the parameter is insignificant concerning the response (Fernández-López *et al.,* 2019).

5.3 Catalyst regeneration

Catalyst regeneration and reusability study were done to ensure industrial feasibility as discussed in Section 3.6.

ODS run was performed under the optimized reaction parameters obtained from the process parameter study. The spent catalyst was filtered out after the reaction and washed with toluene. The cycle of ODS runs and washing of the catalyst were repeated several times to check the reusability of the spent catalyst.

5.4 Kinetic study

Kinetic study was performed to deeply study the reaction mechanism of the ODS process. The optimum catalyst concluded in Chapter 4 was used to study the reaction kinetics. Please refer to Section 3.5 for a detailed discussion.

5.5 Results and discussion

5.5.1 Optimization of ODS parameters

HPMo/TiTUD-1(0.025) catalyst and hydrogen peroxide were used for the parameter's optimization study. 3D graphs were plotted to determine the effects of interactions between two parameters while keeping the third parameter constant at its mid-value. The effects of temperature, amount of catalyst in oil, and oxidant/sulfur (O/S) molar ratio are shown in Figure 5.1. The central point in the figure is represented by factors where temperature =52.5°C, O/S =6.5, and amount of catalyst in oil= 9wt.%. Figure 5.1a shows that the sulfur removal efficiency rises with increasing O/S ratio and the amount of catalyst. In Figure 5.1b, a rise in temperature and catalyst amount moderately increases the sulfur removal (wt.%) to a certain limit. A significant boost in the sulfur removal (wt.%) is noticed in Figure 5.1c with the O/S ratio. The central point coordinates in 3D plots represent the corresponding optimum parameter values. In this study, HPMo/TiTUD-1 (0.025) catalyst showed its highest sulfur removal rate of 44.3 wt.% when the temperature, catalyst amount, and O/S ratio were kept at 50 °C, 8 wt.% and 6, respectively.
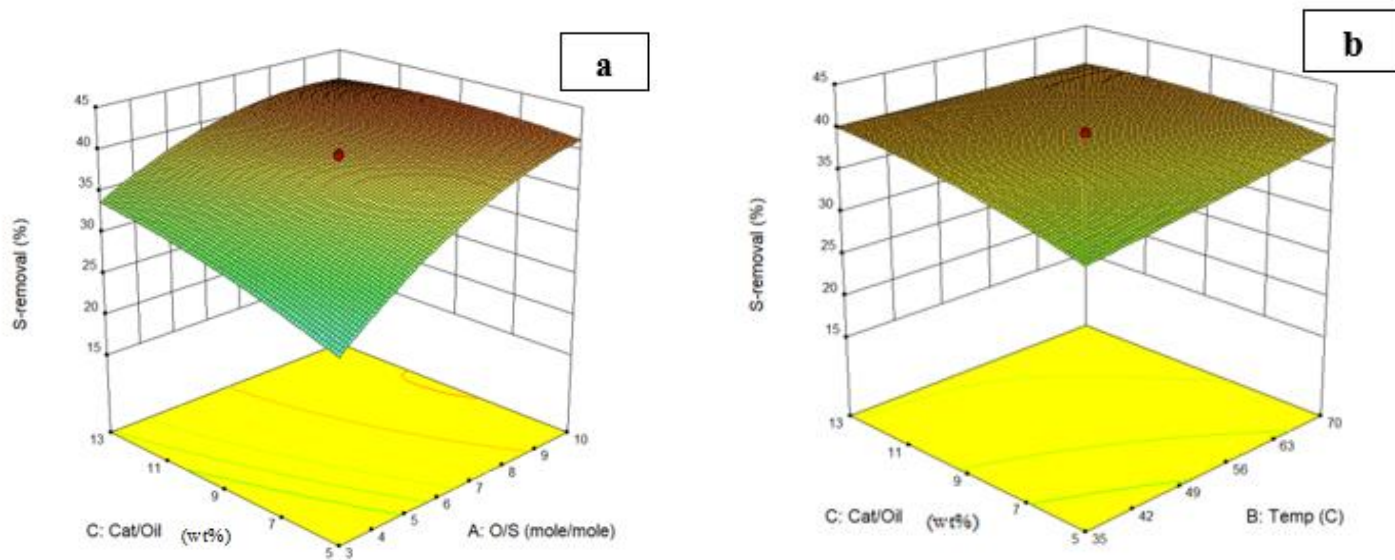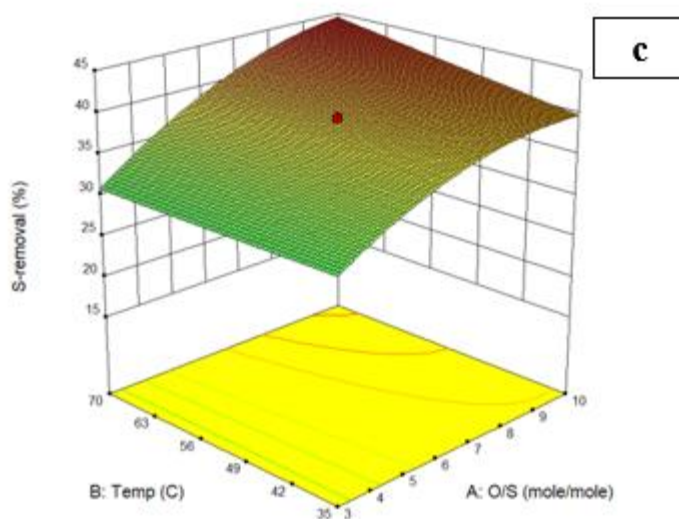
Figure 5. 1 3D response plots: (a) effects of catalyst amount (wt%) and O/S (molar ratio) on sulfur removal, (b) effects of amount of catalyst in oil (wt%) and temperature (°C) on sulfur removal, and (c) effects of temperature (°C) and O/S (molar ratio) on sulfur removal.

5.5.2 Analysis of variance (ANOVA)

Analysis of variance (ANOVA) was done to estimate the impact of process parameters such as temperature, O/S molar ratio, and catalyst amount on sulfur removal. The ANOVA results are given in Table 5.3. The statistical significance of the model was established by F-test and p-test. The model has F and p-values of 9.12, and 0.0009 respectively. These values mean that the model has a high level of fit to experimental data. The p-values of < 0.05 and F-values of > 1.0 indicate that independent variables (A, and C), and quadratic parameters (A^2) are significant. Values greater than 0.1 indicate that model terms are not significant. F-values of individual variables show that the reaction temperature is a statistically less significant factor for the removal of sulfur during ODS of tire pyrolysis oil. The model F-value of 9.12 implies that the model is significant. The model has a standard deviation of 2.79. Furthermore, the coefficient of determination (R^2) value of 0.89 indicates that the model is significant. The "Adeq Precision" measures the signal-to-noise ratio. A ratio greater than 4 is desirable. The ratio of 11.3 for this model indicates an adequate signal.

O/S ratio is found to be the most significant parameter with the F-test value of 54.33 and p-value

<0.0001 followed by the catalyst amount on sulfur removal with comparatively low but still significant F-value of 6.12 and p-value of 0.0329.

Table 5. 3 ANOVA (analysis of variance) for ODS of TPO over HPMo/Ti-TUD-1(0.025) catalyst

Source	Sum of squares	Degree of freedom	Mean square	F value	p-value
Model	638.34	9	70.93	9.12	0.0009
A-O/S	422.28	1	422.28	54.33	<0.0001
B-Temp	18.31	1	18.31	2.36	0.1558
C-Cat/Oil	47.55	1	47.55	6.12	0.0329
AB	12.30	1	12.30	1.58	0.2370
AC	27.16	1	27.16	3.49	0.0911
BC	9.68	1	9.68	1.25	0.2905
A^2	94.15	1	94.15	12.11	0.0059
B^2	0.04	1	0.04	0.01	0.9417
C^2	10.15	1	10.15	1.31	0.2797

Regression analysis of the experimental results showed the best fit to the second-order polynomial shown in equation 5.1 for predicting the sulfur removal performance of HPMo/Ti-TUD-1(0.025) catalyst.

$$\text{S-removal} = 39.08 + 5.56A + 1.16B + 1.87C + 1.24AB - 1.84AC - 1.10BC - 2.56A^2 + 0.06B^2 - 0.84C^2$$

$$(5.1)$$

The equation in terms of coded factors can be used to make predictions about the response for given levels of each factor. By default, the high levels of the factors are coded as +1 and the low level of the factors are coded as -1. The coded equation was useful for identifying the relative impact of the factors by comparing the factor coefficients.

However, if less significant independent variable (B), and quadratic parameters (AB, AC, BC, B^2, and C^2) are eliminated from the model, then the equation of sulfur removal performance of HPMo/Ti-TUD-1(0.025) catalyst can be shown in equation 5.2 and the ANOVA results are given in Table 5.4.

S-removal $= 38.50 + 5.56A + 1.87C - 2.49A^2$ (5.2)

Table 5. 4 Analysis of variance table (ANOVA) for the reduced quadratic model for ODS of TPO over HPMo/Ti-TUD-1(0.025) catalyst

Source	Sum of squares	Degree of freedom	Mean square	F value	p-value
Model	560.45	3	186.82	19.21	<0.0001
A-O/S	422.28	1	422.28	43.42	<0.0001
C-Cat/Oil	47.55	1	47.55	4.89	0.0419
A^2	90.62	1	90.62	9.32	0.0076

5.5.3 Catalyst reusability

The reusability study was done to anticipate the economic feasibility of ODS of tire pyrolysis oil with HPMo/TiTUD-1 (0.025) catalyst. The spent catalyst was washed with toluene, followed by drying in the oven at 100° C for 1 h, and then calcined at 500° C. The catalyst was regenerated after each run. The reusability was tested three times at the optimized condition. The sulfur removal efficiency of the HPMo/TiTUD-1 (0.025) catalyst was gradually dropped by 4-6 wt% after each use as shown in Table 5.5. This is due to the leaching of molybdenum Keggin ions from the surface of TUD-1 by aqueous hydrogen peroxide. This is proved through the XRD patterns of the spent catalyst after 1st and 3rd regenerations compared with the fresh catalyst. As it can be seen from Figure 5.2, all the characteristic peaks of molybdenum Keggin ions gradually decrease after each regeneration, evidencing the leaching of HPMo.

Table 5. 5 Catalyst HPMo/ Ti-TUD-1 (0.025) regeneration data

Catalyst	Sulfur removal (wt.%)	Nitrogen removal (wt.%)
Fresh Catalyst	45.2	79.2
1st regeneration	43.0	77.4
3rd regeneration	38.0	76.1

Moreover, the sulfur removal efficiency can be explained by textural properties data of the fresh catalyst compared with the spent catalyst after 1st and 3rd regeneration. As shown in Table 5.6 the surface area decreases significantly after each regeneration along with pore volume due to the filling of the mesopores with impurities that were not entirely removed by toluene washing and calcination. The moderate desulfurization efficiency obtained was from active sites due to Ti substitution in the catalyst (Vedachalam *et al.,* 2020).
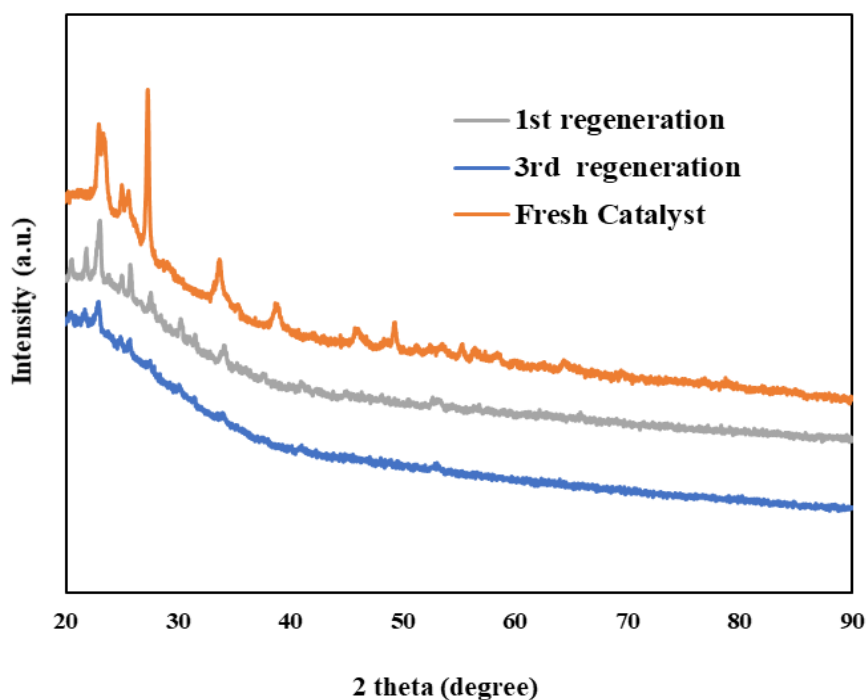
Figure 5. 2 XRD of spent catalyst HPMo/Ti-TUD-1(Ti/Si= 0.025) after regeneration

Table 5. 6 Textural properties of catalyst HPMo/Ti-TUD-1 (0.025)

Sample ID	BET surface area (m²/g)	Pore volume (cm³/g)	BJH pore diameter (nm)
Fresh Catalyst	311	1.2	13.0
1st regeneration	267	1.0	12.6
3rd regeneration	257	0.9	12.6

5.5.4 Kinetics of ODS of tire pyrolysis oil

The ODS of TPO is classified as a three-phase heterogeneous reaction as it includes the oil phase (tire pyrolysis oil), aqueous phase (aqueous hydrogen peroxide), and solid phase (catalyst) (Sengupta *et al.,* 2012). The external mass transfer effects are assumed to be negligible in this study due to a high rate of stirring. Please refer to Figure 2.4 in Section 2.5, where the transfer of oxygen from hydrogen peroxide to sulfur compounds is facilitated by a catalyst to form sulfone and sulfoxide (Houda *et al.,* 2018).

Since hydrogen peroxide is used in excess for ODS, the reaction kinetic is assumed as the zero-order to an oxidant (Kong *et al.,* 2004; Sengupta *et al.,* 2012). The kinetics of oxidative desulfurization reaction over mesoporous catalysts were studied by Chamack et al (Chamack *et al.,* 2014). Oxidation of sulfur into sulfone was found to be a rate-controlling step. The heat transfer and mass transfer limitations were assumed to be insignificant. The surface reactions are shown in equations 5.3 and 5.4:

$$C + * \underset{k_{des}}{\overset{k_{ads}}{\rightleftharpoons}} C*; \text{ reversible adsorption on a catalytic surface} \tag{5.3}$$

$$C* \overset{k_1}{\rightarrow} CO + *; \text{ rate} - \text{limiting step surface reaction} \tag{5.4}$$
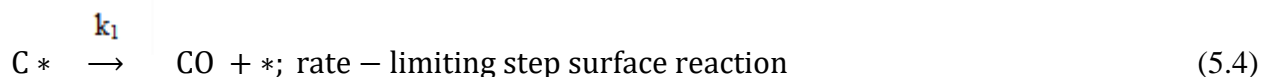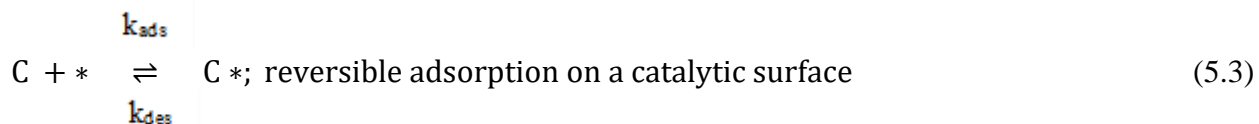
Where C = sulfur compound in TPO, * refers to an activated surface site that adsorbs C and yields C*, and k_1, k_{ads}, k_{des} represents rate constants for surface reaction, adsorption, and desorption

respectively. As shown in equation 5.4, C* is converted to CO which is the rate-limiting step. The rate of reaction (r) could be expressed by considering the Langmuir–Hinshelwood mechanism as shown in equation 5.5:

$$r = k1 \, [C *] \tag{5.5}$$

With the steady-state estimation, the activated intermediate concentration is given as per equation 5.6 as follows:

$$[C *] = kads \, [C][*]/ (kdes + k1) \tag{5.6}$$

If the rate constant is termed as shown in equation 5.7:

$$[k] = k1 \, kdes \, [*]/ (kdes + k1) \tag{5.7}$$

The rate of the equation is represented by the following equation 5.8:

$$r = k \, [C] \tag{5.8}$$

So, the ODS reaction is pseudo-first order to [C]. If $[C]_0$: concentration of C at t = 0 and $[C]_t$: concentration of C at t = t, the reaction rate constant (k) can be expressed by equation 5.9:

$$Ln \, ([C]0/[C]t) = kt \tag{5.9}$$

The plot of ln ($[C]_0/[C]_t$) versus the reaction time provides the rate constant. In this study, kinetic of ODS of TPO was explored over HPMo/TiTUD-1 (0.025) catalyst at different run times: 15, 30, 60, and 120 min. The plot of Ln ($[C]0/[C]t$) represented by 'y' versus the run time represented by 'x' in the equation is shown in Figure 5.4. The kinetic data fit well to the pseudo-first-order kinetic rate. Value of rate constant k as depicted from the slope of the line which is 0.0004 min^{-1}. Furthermore, the R^2 value of 0.96 proves that the pseudo-first-order model fits quite well. The previous studies on the catalytic oxidation of sulfur compounds of fuel oils have reported that ODS typically follows the pseudo-first-order reaction (Houda *et al.,* 2018; Vedachalam *et al.,* 2020).
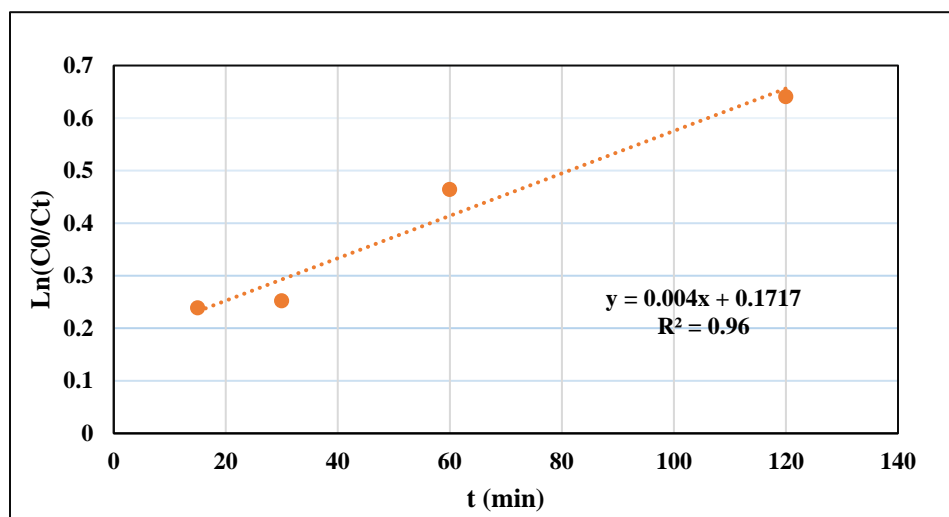
Figure 5. 3 Pseudo first-order kinetics of ODS runs with HPMo/Ti-TUD-1(0.025) catalyst; catalyst/feed ratio=0.05; T=70 °C; oxidant, 30% H_2O_2; H_2O_2/S=10; and stirring=550 rpm.

5.6 Conclusions

In this phase of the research process parameters such as temperature, amount of catalyst in oil, and oxidant/sulfur (O/S) were evaluated using a central composite design. In the process parameters study, HPMo/TiTUD-1 (0.025) catalyst showed its highest sulfur removal rate of 44.3 wt.% at the temperature, cat/oil, and O/S of 50 °C, 8 wt.% and 6 respectively. As per ANOVA, the O/S ratio and amount of catalyst loading in oil are the most significant parameters in terms of sulfur removal efficiency. The interaction of the process parameters with each other is not that significant as compared to their individual effects. The results of the catalyst regeneration study show that the catalyst, HPMo/TiTUD-1 (0.025), can be reused at least three times with a marginal loss in sulfur removal efficiency. The sulfur removal efficiency decreases due to the leaching of HPMo from the catalyst surface in the presence of H_2O_2 after every run. The minimal sulfur efficiency obtained during the regeneration study is due to unaltered active sites present in the catalyst. The decrease in the BET surface area and the pore volume was observed due to the filling of the mesopores with impurities. Kinetics parameters most likely reflect that the key step in the oxidation of sulfur refractory compounds involves both catalyst and sulfur compounds in the feed. In the end, the kinetic study of ODS concludes the order of rate of reaction to be pseudo-first order.

Chapter 6: Summary, conclusions, and recommendations

6.1 Summary

This research focused on the desulfurization of tire pyrolysis oil as per the environmental standards through the oxidative desulfurization technique. In the first phase of this research work, mesoporous alumina and TUD-1 supports were prepared with the incorporation of Ti. Impregnation of phosphomolybdic acid was done for the preparation of a series of catalysts with different Ti/Al and Ti/Si ratios. Characterization of prepared catalysts was conducted using various analyzers and studied thoroughly. This was followed by subsequent ODS screening tests to find the optimized catalyst and oxidant that provided the highest sulfur removal efficiency (wt.%). The second phase of the research included the process parameter optimization using the optimized catalyst concluded from the previous research phase using central composite design software. The ODS kinetic study at different temperatures was performed to find rate the rate of the reaction. Catalyst regeneration was examined using the optimized catalyst at the optimum process parameters to determine the maximum utilization of the spent catalyst.

6.2 Overall conclusions

Phosphomolybdic acid-loaded titania-incorporated mesoporous Al_2O_3 and TUD-1 catalysts were successfully prepared and evaluated for the catalytic oxidation desulfurization of tire pyrolysis oil at mild process conditions. XRD results substantiate that HPMo retained its Keggin structure in the TUD-1 supported catalysts, whereas it suffered decomposition in the Al_2O_3 supported catalysts. The XPS characterization results evidenced the successful incorporation of Ti into the Al_2O_3 and TUD-1 frameworks. Pyridine FTIR results authenticated the presence of both Brønsted and Lewis acid sites in HPMo/Ti-Al_2O_3 and HPMo/Ti-TUD-1 catalysts. Titanium evidenced a promotional effect on the ODS activity of phosphomolybdic acid. Among the two series of catalysts, HPMo/Ti-TUD-1(0.025) was found to be the most active catalyst for ODS of tire pyrolysis oil with 45.2 wt% of sulfur removal efficiency. As per ANOVA statistical study, the reaction temperature was found to be a less significant factor than the concentrations of oxidant and catalyst for promoting ODS of tire pyrolysis oil. The sulfur oxidation on HPMo/Ti-TUD-1(0.025) followed the pseudo-first-order kinetics with the R^2 value of 0.96. The results of the

catalyst regeneration study show that the catalyst can be reused at least three times with a marginal loss in sulfur removal efficiency.

6.3 Recommendations

- The activity of the catalyst in a continuous mode needs to be explored.
- Textural properties (BET surface area, pore-volume, and pore diameter) of the prepared catalysts can be improved by changing the synthesis process conditions such as calcination temperature for better catalytic activity.
- The incorporation of linkers with the support can be studied to avoid the leaching of molybdenum Keggin ions from the surface of the catalyst.
- In this study, during solvent extraction, sulfones and sulfoxides were dissolved in the solvent and the desulfurized tire pyrolysis oil was separated as the product. The solvent can be reused again by removing the dissolved oxidized sulfur species by rotary evaporation.
- Furthermore, proper waste management or finding the reuse of the removed sulfones and sulfoxides by rotary evaporator, that can be either directly used as a raw material or processed for its usage as feed in some other process. For example, sulfones can be further used for their medicinal effect.
- Oxidative desulfurization can be served as a secondary treatment to hydrodesulfurization to remove the last few remaining ppm of sulfur compounds to ensure maximum efficiency.
- And lastly, the techno-economic analysis can be studied for the whole process to check if the whole process is industrially viable and feasible.

7. References

Mohammed, D. M., Isah, A. G., Musa, U., Shehu, A., & Abdullahi, Y. N. (2012). Comparative study on sulphur reduction from heavy petroleum-Solvent extraction and microwave irradiation approach. International Journal of Energy and Environment, 3 (6), 949–60.

Abubakar, A., Mohammed-Dabo, I. A., & Ahmed, A. S. (2016). Reduction of Sulphur Content of Urals Crude Oil Prior To Processing Using Oxidative Desulphurization. Nigerian Journal of Basic and Applied Sciences, 24(1), 19-24.

Afzalinia, A., Mirzaie, A., Nikseresht, A. and Musabeygi, T. 2017. "Ultrasonics Sonochemistry Ultrasound-Assisted Oxidative Desulfurization Process of Liquid Fuel by Phosphotungstic Acid Encapsulated in a Interpenetrating Amine-Functionalized Zn (II) -Based MOF as Catalyst." Ultrasonics - Sonochemistry, 34, 713–20.

Ahmad, S., Ahmad, M. I., Naeem, K., Humayun, M., & Faheem, F. (2016). Oxidative desulfurization of tire pyrolysis oil. Chemical Industry and Chemical Engineering Quarterly, 22(3), 249-254.

Al-Lal, A. M., Bolonio, D., Llamas, A., Lapuerta, M., & Canoira, L. (2015). Desulfurization of pyrolysis fuels obtained from waste: Lube oils, tires and plastics. Fuel, 150, 208-216.

Alsaleh, A., & Sattler, M. L. (2014). Waste tire pyrolysis: influential parameters and product properties. Current Sustainable/Renewable Energy Reports, 1(4), 129-135.

"Automotive." 2021. TechSci Research. 2021. https://www.techsciresearch.com/report/canada-tire-market/4036.html. Accessed on 4 July 2021.

Badoga, S., Misra, P., Kamath, G., Zheng, Y., & Dalai, A. K. (2018). Hydrotreatment Followed by oxidative desulfurization and denitrogenation to attain low sulphur and nitrogen bitumen derived gas oils. Catalysts, 8(12), 645.

Badoga, S., Sharma, R. V., Dalai, A. K., & Adjaye, J. (2014). Hydrotreating Of Heavy Gas oil on mesoporous mixed metal oxides (M–Al_2O_3, M= TiO_2, ZrO_2, SnO_2) supported NiMo catalysts: Influence of surface acidity. Industrial & Engineering Chemistry Research, 53(49), 18729-18739.

Bazyari, A., Khodadadi, A. A., Mamaghani, A. H., Beheshtian, J., Thompson, L. T., & Mortazavi, Y. (2016). Microporous titania–silica nanocomposite catalyst-adsorbent for ultra-deep oxidative desulfurization. Applied Catalysis B: Environmental, 180, 65-77.

Bockstal, L., Berchem, T., Schmetz, Q., & Richel, A. (2019). Devulcanisation and reclaiming of

tires and rubber by physical and chemical processes: A review. Journal of Cleaner Production, 236, 117574.

Bunthid, D., Prasassarakich, P., & Hinchiranan, N. (2010). Oxidative desulfurization of tire pyrolysis naphtha in formic acid/H2O2/pyrolysis char system. Fuel, 89(9), 2617-2622.

Cedeño-Caero, L., Ramos-Luna, M., Méndez-Cruz, M., & Ramírez-Solís, J. (2011). Oxidative desulfurization of dibenzothiophene compounds with titania based catalysts. Catalysis today, 172(1), 189-194.

Čejka, J. (2003). Organized mesoporous alumina: synthesis, structure and potential in catalysis. Applied Catalysis A: General, 254(2), 327-338.

Chamack, M., Mahjoub, A. R., & Aghayan, H. (2014). Cesium salts of tungsten-substituted molybdophosphoric acid immobilized onto platelet mesoporous silica: Efficient catalysts for oxidative desulfurization of dibenzothiophene. Chemical Engineering Journal, 255, 686-694.

Cho, K. S., & Lee, Y. K. (2014). Effects of nitrogen compounds, aromatics, and aprotic solvents on the oxidative desulfurization (ODS) of light cycle oil over Ti-SBA-15 catalyst. Applied Catalysis B: Environmental, 147, 35-42.

Choi, A. E. S., Roces, S., Dugos, N., Futalan, C. M., Lin, S. S., & Wan, M. W. (2014). Optimization of ultrasound-assisted oxidative desulfurization of model sulfur compounds using commercial ferrate (VI). Journal of the Taiwan Institute of Chemical Engineers, 45(6), 2935-2942.

Choi, A. E. S., Roces, S., Dugos, N., & Wan, M. W. (2016). Oxidation by H2O2 of benzothiophene and dibenzothiophene over different polyoxometalate catalysts in the frame of ultrasound and mixing assisted oxidative desulfurization. Fuel, 180, 127-136.

Cruz, P., Granados, E. A., Fajardo, M., del Hierro, I., & Pérez, Y. (2019). Heterogeneous oxidative desulfurization catalysed by titanium grafted mesoporous silica nanoparticles containing tethered hydrophobic ionic liquid: A dual activation mechanism. Applied Catalysis A: General, 587, 117241.

Cui, Z., Feng, X., Li, H., & Tan, T. (2020). Interconversion of Lewis acid and Brønsted acid catalysts in biomass-derived paraxylene synthesis. Chemical Engineering Science, 227, 115942.

"Current World Population." 2021. Worldometer. 2021. https://www.worldometers.info/world-population/. Accessed on 10 September 2021.

de Luna, M. D. G., Samaniego, M. L., Ong, D. C., Wan, M. W., & Lu, M. C. (2018). Kinetics of sulfur removal in high shear mixing-assisted oxidative-adsorptive desulfurization of diesel. Journal of Cleaner Production, 178, 468-475.

Dedual, G., MacDonald, M. J., Alshareef, A., Wu, Z., Tsang, D. C., & Yip, A. C. (2014). Requirements for effective photocatalytic oxidative desulfurization of a thiophene-containing solution using TiO$_2$. Journal of Environmental Chemical Engineering, 2(4), 1947-1955.

Dhir, S., Uppaluri, R., & Purkait, M. K. (2009). Oxidative desulfurization: Kinetic modelling. Journal of hazardous materials, 161(2-3), 1360-1368.

Ding, W., Zhu, W., Xiong, J., Yang, L., Wei, A., Zhang, M., & Li, H. (2015). Novel heterogeneous iron-based redox ionic liquid supported on SBA-15 for deep oxidative desulfurization of fuels. Chemical Engineering Journal, 266, 213-221.

Doğan, O., Çelik, M. B., & Özdalyan, B. (2012). The effect of tire derived fuel/diesel fuel blends utilization on diesel engine performance and emissions. Fuel, 95, 340-346.

Estephane, G., Lancelot, C., Blanchard, P., Toufaily, J., Hamiye, T., & Lamonier, C. (2018). Sulfur compounds reactivity in the ODS of model and real feeds on W–SBA based catalysts. RSC advances, 8(25), 13714-13721.

Farshi, A., & Shiralizadeh, P. (2015). Sulfur reduction of heavy fuel oil by oxidative desulfurization method. Petroleum & Coal, 57(3).

Fernández-López, J. A., Angosto, J. M., Roca, M. J., & Miñarro, M. D. (2019). Taguchi design-based enhancement of heavy metals bioremoval by agroindustrial waste biomass from artichoke. Science of the Total Environment, 653, 55-63.

Fogler, H. S. (2004). *Elements of Chemical Reaction Engineering*. 3rd Edition, 967.

Fraile, J. M., Gil, C., Mayoral, J. A., Muel, B., Roldán, L., Vispe, E., Calderón, S. & Puente, F. (2016). Heterogeneous titanium catalysts for oxidation of dibenzothiophene in hydrocarbon solutions with hydrogen peroxide: On the road to oxidative desulfurization. Applied Catalysis B: Environmental, 180, 680-686.

Ghubayra, R., Nuttall, C., Hodgkiss, S., Craven, M., Kozhevnikova, E. F., & Kozhevnikov, I. V. (2019). Oxidative desulfurization of model diesel fuel catalyzed by carbon-supported heteropoly acids. Applied Catalysis B: Environmental, 253, 309-316.

Gürü, M. (2007). Oxidative desulfurization of aşkale coal by nitric acid solution. Energy Sources, Part A, 29(5), 463-469.

Guth, E., & Diaz, A. (1974). U.S. Patent No. 3,847,800. Washington, DC: U.S. Patent and Trademark Office.

Haghighat Mamaghani, A., Fatemi, S., & Asgari, M. (2013). Investigation of influential parameters in deep oxidative desulfurization of dibenzothiophene with hydrogen peroxide and formic acid. International Journal of Chemical Engineering, 2013.

Holder, C. F., & Schaak, R. E. (2019). Tutorial on powder X-ray diffraction for characterizing nanoscale materials.

Hossain, M. N., Park, H. C., & Choi, H. S. (2019). A comprehensive review on catalytic oxidative desulfurization of liquid fuel oil. Catalysts, 9(3), 229.

Houda, S., Lancelot, C., Blanchard, P., Poinel, L., & Lamonier, C. (2018). Oxidative desulfurization of heavy oils with high sulfur content: a review. Catalysts, 8(9), 344.

"IMO 2020." 2019. International Maritime Organization. 2019. https://www.imo.org/en/MediaCentre/HotTopics/Pages/Sulphur-2020.aspx. Accessed on 22 January 2019.

Islam, M. N., & Nahian, M. R. (2016). Improvement of waste tire pyrolysis oil and performance test with diesel in CI Engine. Journal of Renewable Energy, 2016.

Javadli, R., & De Klerk, A. (2012). Desulfurization of heavy oil. Applied petrochemical research, 1(1), 3-19.

Jiang, W., Zhu, W., Li, H., Chao, Y., Xun, S., Chang, Y., ... & Zhao, Z. (2014). Mechanism and optimization for oxidative desulfurization of fuels catalyzed by Fenton-like catalysts in hydrophobic ionic liquid. Journal of Molecular Catalysis A: Chemical, 382, 8-14.

Jin, W., Tian, Y., Wang, G., Zeng, D., Xu, Q.,and Cui., J. (2017). Ultra-Deep Oxidative Desulfurization of Fuel with H2O2 Catalyzed by Molybdenum Oxide Supported on Alumina Modified by Ca2+. RSC Advances, 7 (76), 48208–13.

Díaz de León, J. N., Ramesh Kumar, C., Antúnez-García, J., & Fuentes-Moyado, S. (2019). Recent insights in transition metal sulfide hydrodesulfurization catalysts for the production of ultra low sulfur diesel: A short review. Catalysts, 9(1), 87.

Jose, N., Sengupta, S., & Basu, J. K. (2011). Optimization of oxidative desulfurization of thiophene using Cu/titanium silicate-1 by box-behnken design. Fuel, 90(2), 626-632.

Juma, M., Koreňová, Z., Markoš, J., Jelemensky, L., & Bafrnec, M. (2007). Experimental study of pyrolysis and combustion of scrap tire. Polymers for Advanced Technologies, 18(2), 144-

148.

Kazakov, A. A., Tarakanov, G. V., & Ionov, N. G. (2016). Mechanisms of oxidative desulfurization of straight-run residual fuel oil using ozonized air. Chemistry and Technology of Fuels and Oils, 52(1), 33-37.

Kong, L., Li, G., & Wang, X. (2004). Kinetics and mechanism of liquid-phase oxidation of thiophene over TS-1 using H_2O_2 under mild conditions. Catalysis Letters, 92(3), 163-167.

Krivtsov, E. B., & Golovko, A. K. (2014). The kinetics of oxidative desulfurization of diesel fraction with a hydrogen peroxide-formic acid mixture. Petroleum Chemistry, 54(1), 51-57.

Laresgoiti, M. F., Caballero, B. M., de Marco, I., Torres, A., Cabrero, M. A., & Chomón, M. J. (2004). Characterization of the liquid products obtained in tyre pyrolysis. Journal of Analytical and Applied Pyrolysis, 71(2), 917-934.

Lesaint, C., Glomm, W. R., Borg, Ø., Eri, S., Rytter, E., & Øye, G. (2008). Synthesis and characterization of mesoporous alumina with large pore size and their performance in Fischer–Tropsch synthesis. Applied Catalysis A: General, 351(1), 131-135.

Marosi, L., Platero, E. E., Cifre, J., & Areán, C. O. (2000). Thermal dehydration of $H_{3+}xPVxM_{12-}xO_{40}\cdot yH_2O$ Keggin type heteropolyacids; formation, thermal stability and structure of the anhydrous acids H3PM12O40, of the corresponding anhydrides PM12O38. 5 and of a novel trihydrate $H3PW12O40\cdot 3H2O$Present address: Leuschnerstr. 32, 67063 Ludwigshafen, Germany. Journal of Materials Chemistry, 10(8), 1949-1955.

Martínez, J. D., Puy, N., Murillo, R., García, T., Navarro, M. V., & Mastral, A. M. (2013). Waste tyre pyrolysis–A review. Renewable and sustainable energy reviews, 23, 179-213.

Mastral, A. M., Murillo, R., Callen, M. S., & Garcia, T. (2000). Optimisation of scrap automotive tyres recycling into valuable liquid fuels. Resources, Conservation and Recycling, 29(4), 263-272.

Matalon, Lorne. 1990. "1990: The Hagersville Tire Fire." *CBC Digital*. Canada. https://www.cbc.ca/archives/entry/1990-the-hagersville-tire-fire%0D. Accessed on 15 June 2019.

Mushrush, G. W., Beal, E. J., Pellenbarg, R. E., Hazlett, R. N., Eaton, H. R., & Hardy, D. R. (1994). A model study of the thermal decomposition of cumene hydroperoxide and fuel instability reactions. Energy & fuels, 8(4), 851-855.

Ogunlaja, A. S., Alade, O. S., & Tshentu, Z. R. (2017). Vanadium (IV) catalysed oxidation of

organosulfur compounds in heavy fuel oil. Comptes Rendus Chimie, 20(2), 164-168.

Rana, R., Badoga, S., Dalai, A. K., & Adjaye, J. (2017). The impact of process parameters on the deposition of fines present in bitumen-derived gas oil on hydrotreating catalyst. Energy & Fuels, 31(6), 5969-5981.

Rivoira, L. P., Valles, V. A., Ledesma, B. C., Ponte, M. V., Martinez, M. L., Anunziata, O. A., & Beltramone, A. R. (2016). Sulfur elimination by oxidative desulfurization with titanium-modified SBA-16. Catalysis Today, 271, 102-113.

Saleh, T. A., & Danmaliki, G. I. (2016). Adsorptive desulfurization of dibenzothiophene from fuels by rubber tyres-derived carbons: kinetics and isotherms evaluation. Process Safety and Environmental Protection, 102, 9-19.

Schnecko, H. (1998). Rubber recycling. Macromolecular Symposia, 135(1), 327-343.

Sengupta, A., Kamble, P. D., Basu, J. K., & Sengupta, S. (2012). Kinetic study and optimization of oxidative desulfurization of benzothiophene using mesoporous titanium silicate-1 catalyst. Industrial & engineering chemistry research, 51(1), 147-157.

Serefentse, R., Ruwona, W., Danha, G., & Muzenda, E. (2019). A review of the desulphurization methods used for pyrolysis oil. Procedia Manufacturing, 35, 762-768.

Shan, Z., Gianotti, E., Jansen, J. C., Peters, J. A., Marchese, L., & Maschmeyer, T. (2001). One-step synthesis of a highly active, mesoporous, titanium-containing silica by using bifunctional templating. Chemistry-A European Journal, 7(7), 1437-1443.

Shen, C., Wang, Y. J., Xu, J. H., & Luo, G. S. (2016). Oxidative desulfurization of DBT with H_2O_2 catalysed by TiO_2/porous glass. Green Chemistry, 18(3), 771-781.

"Short-Term Energy Outlook." 2021. U.S Energy Information Administration. 2021. Accessed May 2021.

Sinha, A. K., Seelan, S., Okumura, M., Akita, T., Tsubota, S., & Haruta, M. (2005). Three-dimensional mesoporous titanosilicates prepared by modified sol-gel method: Ideal gold catalyst supports for enhanced propene epoxidation. The Journal of Physical Chemistry B, 109(9), 3956-3965.

Takallou, H Barry. 2015. "Waste Tire Management." Accessed on 22 September 2021.

Tang, L., Luo, G., Zhu, M., Kang, L., & Dai, B. (2013). Preparation, characterization and catalytic performance of HPW-TUD-1 catalyst on oxidative desulfurization. Journal of Industrial and Engineering Chemistry, 19(2), 620-626.

Tang, Q., Lin, S., Cheng, Y., Liu, S., & Xiong, J. R. (2013). Ultrasound-assisted oxidative desulfurization of bunker-C oil using tert-butyl hydroperoxide. Ultrasonics sonochemistry, 20(5), 1168-1175.

Telalović, S., Ramanathan, A., Mul, G., & Hanefeld, U. (2010). TUD-1: synthesis and application of a versatile catalyst, carrier, material…. Journal of materials chemistry, 20(4), 642-658.

"Tire Derived Fuel." 2020. Cision. 2020. https://www.prnewswire.com/news-releases/worldwide-tire-derived-fuel-market-to-2027. Accessed on 14 September 2020.

Toteva, V., Georgiev, A., & Topalova, L. (2009). Oxidative desulphurization of light cycle oil: Monitoring by FTIR spectroscopy. Fuel Processing Technology, 90(7-8), 965-970.

Vedachalam, S., Boahene, P., & Dalai, A. K. (2020). Oxidative desulfurization of heavy gas oil over a Ti–TUD-1-Supported Keggin-type molybdenum heteropolyacid. Energy & Fuels, 34(12), 15299-15312.

Van Veen, J. A. R., Hendriks, P. A. J. M., Andrea, R. R., Romers, E. J. G. M., & Wilson, A. E. (1990). Chemistry of phosphomolybdate adsorption on alumina surfaces. 2. The molybdate/phosphated alumina and phosphomolybdate/alumina systems. Journal of Physical Chemistry, 94(13), 5282-5285.

Wang, D., Qian, E. W., Amano, H., Okata, K., Ishihara, A., & Kabe, T. (2003). Oxidative desulfurization of fuel oil: Part I. Oxidation of dibenzothiophenes using tert-butyl hydroperoxide. Applied Catalysis A: General, 253(1), 91-99.

Wang, S. S., & Yang, G. Y. (2015). Recent advances in polyoxometalate-catalyzed reactions. Chemical reviews, 115(11), 4893-4962.

Wei, S., He, H., Cheng, Y., Yang, C., Zeng, G., & Qiu, L. (2016). Performances, kinetics and mechanisms of catalytic oxidative desulfurization from oils. RSC advances, 6(105), 103253-103269.

Williams, P. T., & Brindle, A. J. (2002). Catalytic pyrolysis of tyres: influence of catalyst temperature. Fuel, 81(18), 2425-2434.

"Worldwide Tire Industry." 2021. Business Wire. 2021. https://www.businesswire.com/news/home/20210706005425/en/Worldwide-Tire-Industry-to-2026. Accessed on 7 March 2021.

Xia, Z., Fu, J., Duan, A., Han, L., Wu, H., Zhao, Z., ... & Meng, Q. (2017). Post synthesis of aluminum modified mesoporous TUD-1 materials and their application for FCC diesel

hydrodesulfurization catalysts. Catalysts, 7(5), 141.

Yang, S. T., Jeong, K. E., Jeong, S. Y., & Ahn, W. S. (2012). Synthesis of mesoporous TS-1 using a hybrid SiO_2–TiO_2 xerogel for catalytic oxidative desulfurization. Materials Research Bulletin, 47(12), 4398-4402.

Zeelani, G. G., & Pal, S. L. (2016). A review on desulfurization techniques of liquid fuels. Int J Sci Res, 5, 2413-2419.

Zhang, Q., Zhu, M., Jones, I., Zhang, Z., & Zhang, D. (2020). Desulfurization of spent tire pyrolysis oil and its distillate via combined catalytic oxidation using H_2O_2 with formic acid and selective adsorption over Al_2O_3. Energy & Fuels, 34(5), 6209-6219.

Zheng, D., Zhu, W., Xun, S., Zhou, M., Zhang, M., Jiang, W., ... & Li, H. (2015). Deep oxidative desulfurization of dibenzothiophene using low-temperature-mediated titanium dioxide catalyst in ionic liquids. Fuel, 159, 446-453.

Appendix A: Additional results

Table A. 1 Additional design of experiment with results for process optimization

Run	Factor 1 O/S (molar ratio)	Factor 2 Run temperature (°C)	Factor 3 Amount of catalyst in oil (wt%)	Response 1 S-removal (wt%)	Response 2 N-removal (wt%)
1	3.0	35.0	13.0	37.9	74.6
2	6.5	52.5	9.0	39.3	74.5
3	6.5	52.5	15.7	39.6	78.7
4	3.0	35.0	5.0	29.1	68.0
5	10.0	35.0	13.0	39.9	75.8
6	6.5	81.9	9.0	41.4	73.3
7	10.0	70.0	13.0	41.3	77.7
8	0.6	52.5	9.0	17.8	80.7
9	6.5	52.5	2.3	30.6	78.8
10	6.5	52.5	9.0	38.7	81.7
11	12.4	52.5	9.0	42.7	82.5
12	6.5	23.1	9.0	33.9	79.7
13	6.5	52.5	9.0	39.6	82.6
14	6.5	52.5	9.0	39.0	78.0
15	6.5	52.5	9.0	39.3	80.3
16	10.0	35.0	5.0	39.1	78.3
17	10.0	70.0	5.0	44.3	78.8
18	3.0	70.0	5.0	30.0	78.0
19	3.0	70.0	13.0	33.7	83.0
20	6.5	52.5	9.0	39.2	79.2
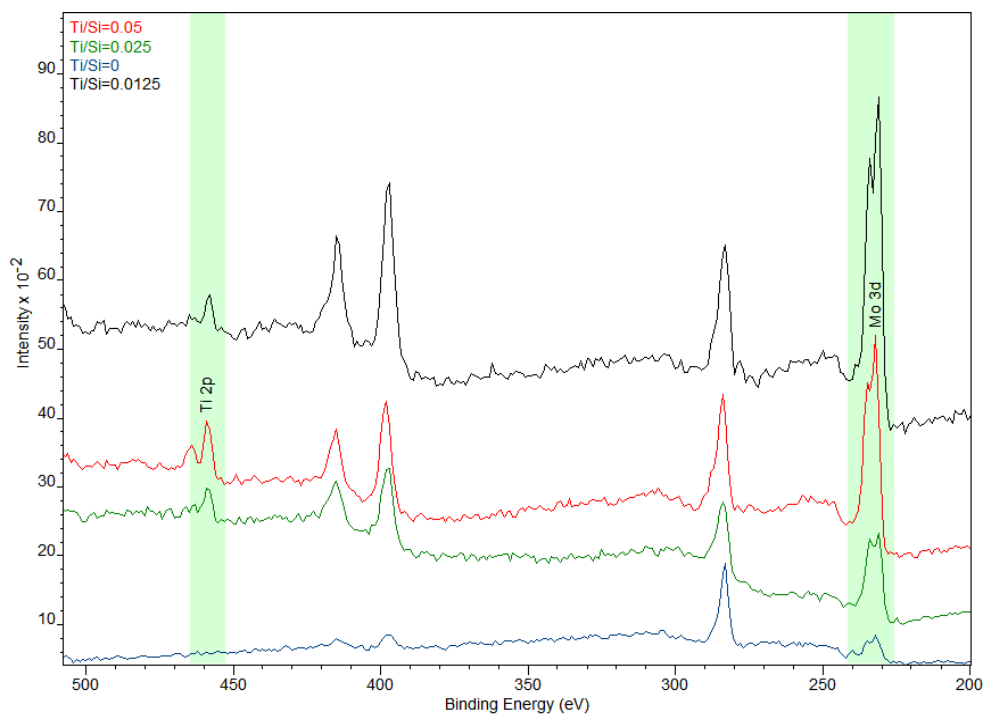
Figure A. 1 Wide scan XPS survey of prepared HPMo/Ti-TUD-1 catalysts
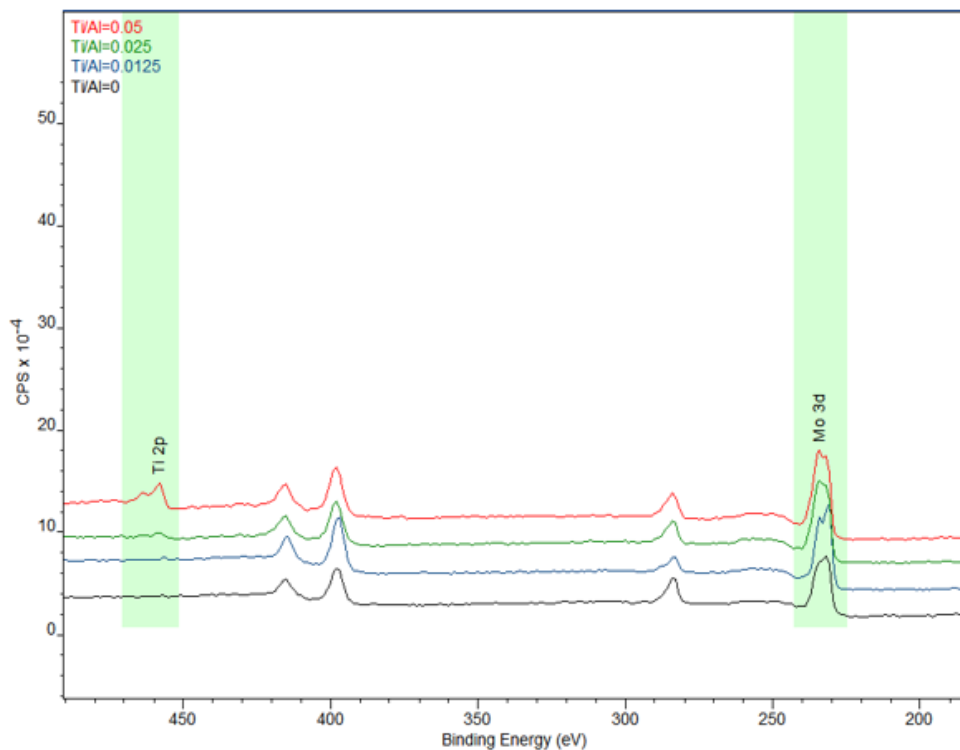
Figure A. 2 Wide scan XPS survey of prepared HPMo/Ti-Al$_2$O$_3$ catalysts

Table A. 2 Removal efficiency data with different HPMo loadings

Catalyst	S- Removal Efficiency (wt%)	N-Removal Efficiency (wt%)
Ti-TUD-1(0.025)	36.9	70.9
10%HPMo/Ti-TUD-1(0.025)	42.6	73.4
20%HPMo/Ti-TUD-1(0.025)	45.2	79.1
30%HPMo/Ti-TUD-1(0.025)	44.3	80.0
45%HPMo/Ti-TUD-1(0.025)	45.7	77.2
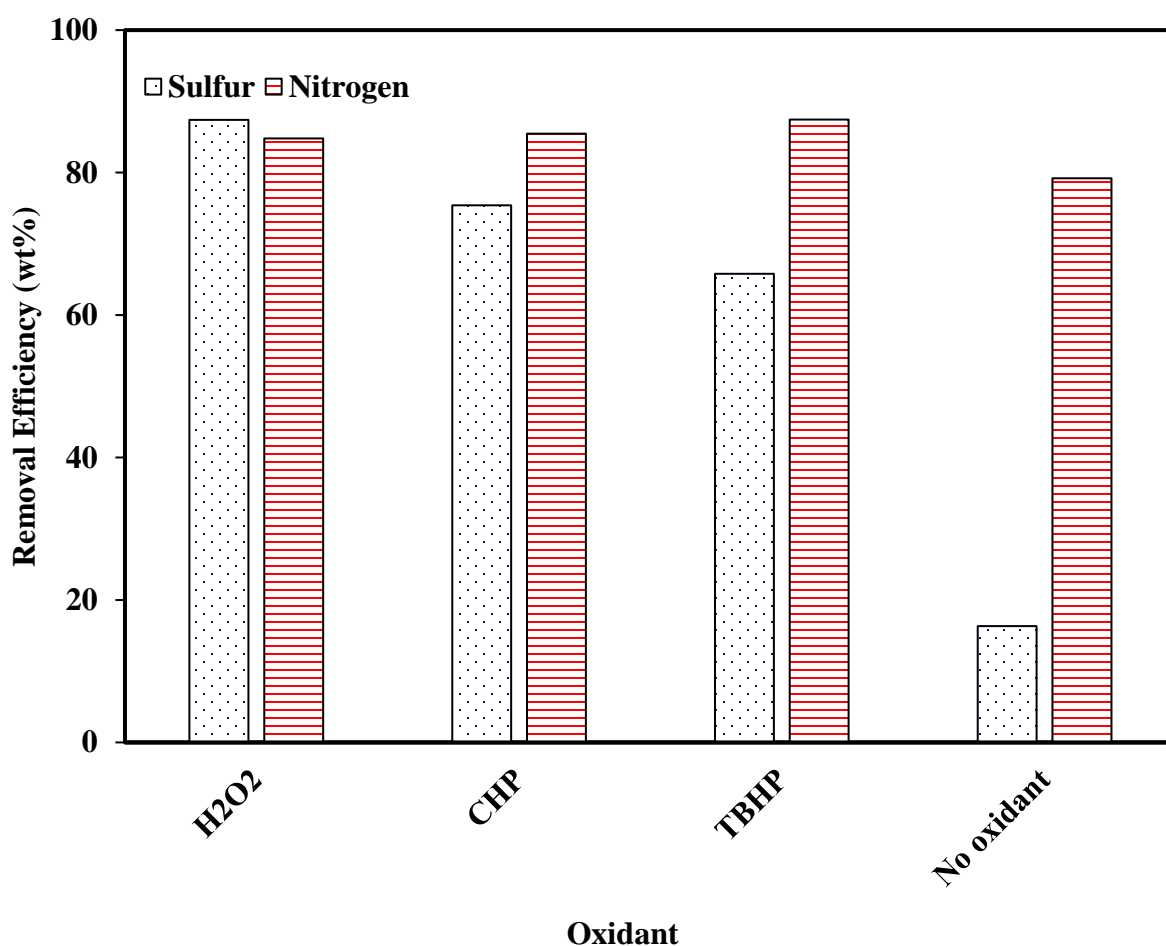
Figure A. 3 Effects of oxidants on ODS of hydrotreated light gas oil over HPMo/Ti-TUD-1 catalyst: catalyst/feed ratio of 0.05; Temperature of 70 °C; Oxidant/Sulfur ratio of 10; reaction time of 2 h; and stirring speed of 550 rpm.

Where CHP: Cumene hydroperoxide; TBHP: tert Butyl hydroperoxide
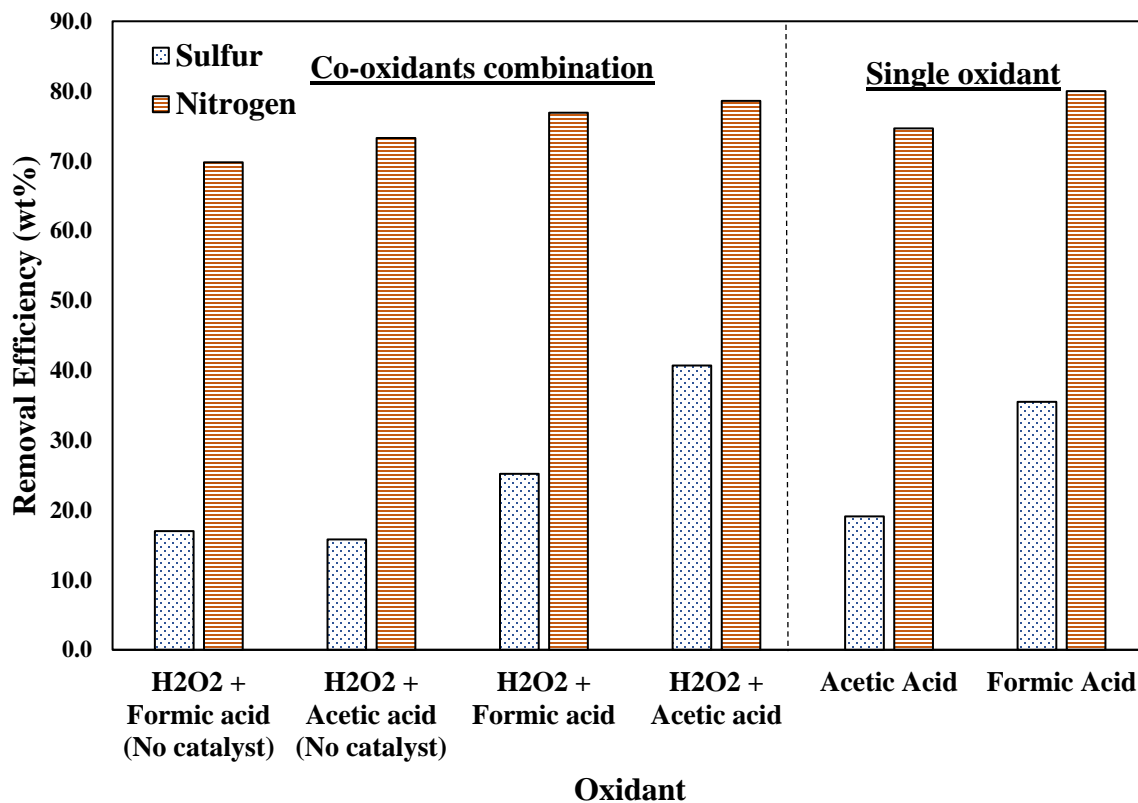
Figure A. 4 Effects of oxidants on ODS activity of TPO with HPMo/TiTUD-1 (0.025) catalyst: catalyst/feed ratio of 0.05; Temperature of 70 °C; Oxidant/Sulfur ratio of 10; reaction time of 2 h; and stirring speed of 550 rpm.
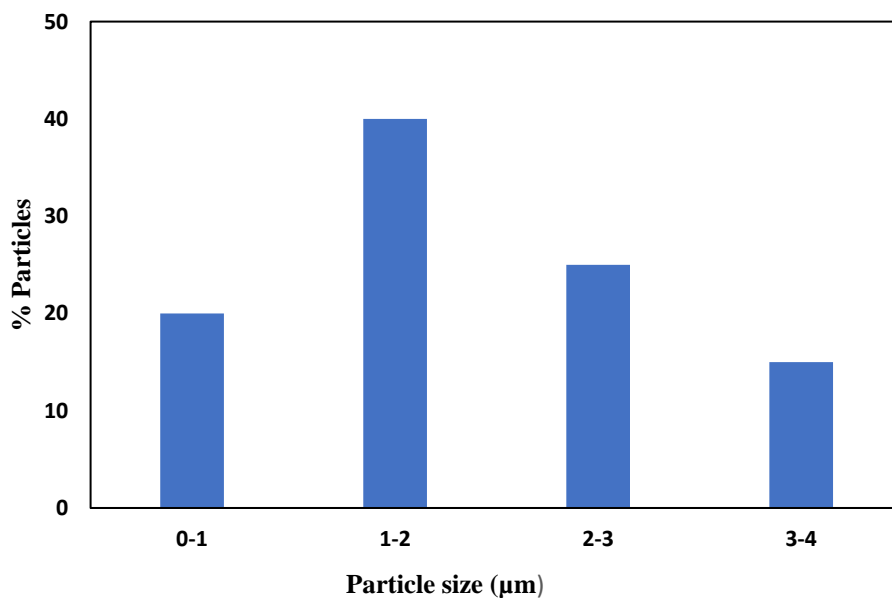
Figure A. 5 Particle size range of particles (%) from SEM image (Figure 4.7(a))

Appendix B: Permission to reuse tables and figures from the submitted paper

Improvement of Waste Tire Pyrolysis Oil and Performance Test with Diesel in CI Engine

M. N. Islam ✉ ⓘ[1] and M. R. Nahian ⓘ[1]

Show more

Academic Editor: Wei-Hsin Chen

Copyright

Under the following terms:

Figure B. 1 Permission to use published article, Table for Chapter 2

Figure B. 2 Permission to use published article, Figure for Chapter 4